
Enhancing the Transferability of Adversarial Examples via a Few Queries

Xiangyuan Yang

Xi'an Jiaotong University
ouyang_xy@stu.xjtu.edu.cn

Jie Lin*

Xi'an Jiaotong University
jielin@mail.xjtu.edu.cn

Hanlin Zhang

Qingdao University
hanlin@qdu.edu.cn

Xinyu Yang

Xi'an Jiaotong University
xyyphd@mail.xjtu.edu.cn

Peng Zhao

Xi'an Jiaotong University
p.zhao@mail.xjtu.edu.cn

Abstract

Due to the vulnerability of deep neural networks, the black-box attack has drawn great attention from the community. Though transferable priors decrease the query number of the black-box query attacks in recent efforts, the average number of queries is still larger than 100, which is easily affected by the number of queries limit policy. In this work, we propose a novel method called query prior-based method to enhance the family of fast gradient sign methods and improve their attack transferability by using a few queries. Specifically, for the untargeted attack, we find that the successful attacked adversarial examples prefer to be classified as the wrong categories with higher probability by the victim model. Therefore, the weighted augmented cross-entropy loss is proposed to reduce the gradient angle between the surrogate model and the victim model for enhancing the transferability of the adversarial examples. Theoretical analysis and extensive experiments demonstrate that our method could significantly improve the transferability of gradient-based adversarial attacks on CIFAR10/100 and ImageNet and outperform the black-box query attack with the same few queries.

1 Introduction

Deep Neural Network (DNN) has penetrated many aspects of life, e.g. autonomous cars, face recognition and malware detection. However, the imperceptible perturbations fool the DNN to make a wrong decision, which is dangerous in the field of security and will cause significant economic losses. To evaluate and increase the robustness of DNN, the advanced adversarial attack methods need to be researched. In recent years, the white-box attacks make a great success and the black-box attacks make great progress. However, because of the weak transferability (with the low attack strength) and the large queries, the black-box attacks can still be further improved.

Recently, a number of transferable prior-based black-box query attacks have been proposed to reduce the number of queries. For example, Cheng et al. [3] proposed a prior-guided random gradient-free (P-RGF) method, which takes the advantage of a transfer-based prior and the query information simultaneously. Yang et al. [42] also proposed a simple baseline approach (SimBA++), which combines transferability-based and query-based black-box attacks, and utilized the query feedback to update the surrogate model in a novel learning scheme. However, the average query number of the most query attacks is larger than 100 in the evaluations on ImageNet. In this scenario, the

*Corresponding author.

performance of these query attacks may be significantly affected when the query number limit policy is applied in the DNN application.

Besides, many black-box transfer attacks have been proposed to enhance the transferability of the adversarial examples, e.g. fast gradient sign method (FGSM) [7], iterative FGSM (I-FGSM) [18], momentum I-FGSM (MI-FGSM) [4], diverse input I-FGSM (DI-FGSM) [39], scale-invariant Nesterov I-FGSM (SI-NI-FGSM) [22] and variance-tuning MI-FGSM (VMI-FGSM) [32]. Zhang et al. [44] also proposed the relative cross-entropy loss (RCE) to enhance the transferability by maximizing the logit’s rank distance from the ground-truth class. However, these transfer attacks achieve weak transferability of adversarial examples under the constraint of low attack strength.

Therefore, to solve the above problems, we propose the query prior-based attacks to enhance the transferability of adversarial examples with few queries under the constraint of low attack strength. Specifically, we find that: (i) The better the transferability of the transfer black-box attack, the smaller the gradient angle between the surrogate model and the victim model. (ii) The successful attacked adversarial examples prefer to be classified as the wrong categories with higher probability by the victim model. Based on the aforementioned findings, the weighted augmented cross-entropy (WACE) loss is proposed to decrease the gradient angle between the surrogate model and the victim model for enhancing the transferability of adversarial examples, which is proved in Appendices A.4 and A.5. The proposed query prior-based method enhances the family of FGSMs by integrating the WACE loss and a few queries. Theoretical analysis and extensive experiments demonstrate that: (i) On the premise of allowing query, the WACE loss is better than cross-entropy (CE) and RCE losses. (ii) Under the constraint of low attack strength, the query prior-based method can significantly improve the family of fast gradient sign methods on CIFAR10/100 [17] and ImageNet [26].

2 Preliminaries

The family of FGSMs and RCE loss are briefly introduced, which is helpful to understand our methods in Section 3 and is regarded as the baselines in Section 4.

2.1 Family of fast gradient sign methods

The methods mentioned in this section are referred as the black-box transfer attacks with the objective of enhancing the transferability of adversarial examples.

Fast gradient sign method (FGSM) [7] is the first transfer attack, which generates the adversarial examples x^{adv} by maximizing the loss function $L(x^{adv}, y_o; \theta)$ with a one-step update:

$$x^{adv} = x + \epsilon \cdot \text{sign}(\nabla_x L(x, y_o; \theta)) \quad (1)$$

where ϵ is the attack strength, y_o is the ground truth, θ is the model parameters, $\text{sign}(\cdot)$ is the sign function and $\nabla_x L(x, y_o; \theta)$ is the gradient of the loss function w.r.t. x .

Iterative FGSM (I-FGSM) [18] is the iterative version of FGSM by applying FGSM with a small step size:

$$x_0 = x, \quad x_{t+1}^{adv} = \text{Clip}_x^\epsilon \{x_t^{adv} + \alpha \cdot \text{sign}(\nabla_x L(x_t^{adv}, y_o; \theta))\} \quad (2)$$

where $\text{Clip}_x^\epsilon(\cdot)$ function restricts generated adversarial examples to be within the ϵ -ball of x .

Momentum I-FGSM (MI-FGSM) [4] integrates the momentum into I-FGSM to escape from poor local maxima and enhance the transferability of adversarial examples:

$$g_{t+1} = \mu \cdot g_t + \frac{\nabla_x L(x_t^{adv}, y_o; \theta)}{\|\nabla_x L(x_t^{adv}, y_o; \theta)\|_1}, \quad (3)$$

$$x_{t+1}^{adv} = \text{Clip}_x^\epsilon \{x_t^{adv} + \alpha \cdot \text{sign}(g_{t+1})\}$$

where g_t is the accumulated gradient at iteration t , and μ is the decay factor of g_t .

Diverse inputs I-FGSM (DI-FGSM) [39] applies random transformations $Tr(\cdot)$ to the input images at each iteration with probability p instead of only using the original images to generate adversarial examples.

Scale-invariant Nesterov I-FGSM (SI-NI-FGSM) [22] integrates Nesterov Accelerated Gradient (NAG) into I-FGSM to leverage the looking ahead property of NAG, i.e. substitutes x_t^{adv} in Eq. 3 with $x_t^{adv} + \alpha \cdot \mu \cdot g_t$, and build a robust adversarial attack. Due to the scale-invariant property of DNN, the scale-invariant attack method is also proposed to optimize the adversarial perturbations over the scale copies of the input images.

Variance tuning MI-FGSM (VMI-FGSM) [32] further considered the gradient variance to stabilize the update direction and escape from the poor local maxima instead of directly using the current gradient for the momentum accumulation:

$$g_{t+1} = \mu \cdot g_t + \frac{\nabla_x L(x_t^{adv}, y_o; \theta) + v_t}{\|\nabla_x L(x_t^{adv}, y_o; \theta) + v_t\|_1}, \quad (4)$$

$$v_{t+1} = \frac{1}{N} \sum_{i=1}^N \nabla_x L(x_{ti}^{adv}, y_o; \theta) - \nabla_x L(x_t^{adv}, y_o; \theta), \quad (5)$$

$$x_{t+1}^{adv} = \text{Clip}_x \{x_t^{adv} + \alpha \cdot \text{sign}(g_{t+1})\}$$

where v_{t+1} is the gradient variance as the t -th iteration, $x_{ti}^{adv} = x_t^{adv} + r_i$, $r_i \sim U[-(\beta \cdot \epsilon)^d, (\beta \cdot \epsilon)^d]$, and $U[a^d, b^d]$ stands for the uniform distribution in d dimensions and β is a hyperparameter.

2.2 Relative cross-entropy (RCE) loss

To escape from the poor local maxima, RCE loss [44] is a new normalized CE loss that guides the logit to be updated in the direction of implicitly maximizing its rank distance from the ground-truth class:

$$L_{CE}(x, y_o; \theta) = -\log \frac{e^{z_o}}{\sum_{c=1}^C e^{z_c}}, \quad (6)$$

$$L_{RCE}(x, y_o; \theta) = L_{CE}(x, y_o; \theta) - \frac{1}{C} \sum_{c=1}^C L_{CE}(x, y_c; \theta) \quad (7)$$

where z_o is the logit of the ground truth label y_o , C is the number of category, y_c is the category with index c .

3 Methodology

In this section, the motivation is introduced firstly. Then, the weighted augmented cross-entropy (WACE) loss is proposed and a corresponding theoretical analysis is described. Finally, our query prior-based method is mentioned, which is generated by combining WACE loss with a few queries.

3.1 Motivation

Though the transferable prior-based black-box query attacks [3, 42] significantly reduce the query number, the average number of queries is still larger than 100. The performance of these query attacks may be greatly affected by the query number limit policy of the DNN applications. On the contrary, we can use the results of a few queries as the priors to enhance the transferability of the black-box transferable attacks. Specifically, we find the preference of the attacked victim model (i.e., Proposition 2). Then a novel black-box transfer attack is designed to achieve higher transferability through the combination of the preference and the results of a few queries.

3.2 Weighted augmented cross-entropy loss

In this section, we first introduce the characteristics and preference of the victim model, and then propose the WACE loss based on the preference and give the theoretical analysis.

For the iterative gradient-based attacks, let f and h denote the surrogate model and the victim model, respectively. We use θ^f and θ^h to denote the parameter of the surrogate model and the victim model, respectively. In the following, Definitions 1 and 2 are mentioned to define the gradient angle between f and h , the top- n wrong categories and the top- n wrong categories attack success rate (ASR) respectively, which are used in the introduction and proof of Propositions 1 and 2 to analyze the preference of the victim model. Propositions 1 and 2 are proved in Appendix A.

Algorithm 1 Query prior-based VMI-FGSM (QVMI-FGSM)

Input: The surrogate model f with parameters θ_f ; the victim model h with parameters θ_h ; the WACE loss L_{WACE} ; an example x with ground truth label y_o ; the magnitude of perturbation ϵ ; the number of iteration T and decay factor μ ; the factor β for the upper bound of neighborhood and the number of example N for variance tuning; the maximum number of queries Q and number of the wrong top- n categories \bar{n} .

Output: An adversarial example x^{adv} .

$$\alpha = \epsilon/T$$

$$g_0 = 0; v_0 = 0; x_0^{adv} = x$$

for $t = 0 \rightarrow T - 1$ **do**

 Query the logit output of the victim model:

$$\mathbf{Z}_h = \begin{cases} h(x_t^{adv}), & \text{if } Q \geq T \\ h(x_t^{adv}), & \text{if } Q < T \wedge t \in \left\{ \lfloor \frac{T}{Q} \rfloor \cdot i \mid i = 0, 1, \dots, Q - 1 \right\} \\ \mathbf{Z}_h, & \text{if } Q < T \wedge t \notin \left\{ \lfloor \frac{T}{Q} \rfloor \cdot i \mid i = 0, 1, \dots, Q - 1 \right\} \end{cases} \quad (8)$$

 Calculate the gradient $g_{t+1} = \nabla_x L_{WACE}(x_t^{adv}, y_o; \theta_f, \mathbf{Z}_h, \bar{n})$

 Update g_{t+1} by variance tuning-based momentum:

$$g_{t+1} = \mu \cdot g_t + \frac{\nabla_x L_{WACE}(x_t^{adv}, y_o; \theta_f, \mathbf{Z}_h, \bar{n}) + v_t}{\|\nabla_x L_{WACE}(x_t^{adv}, y_o; \theta_f, \mathbf{Z}_h, \bar{n}) + v_t\|_1}$$

 Update v_{t+1} by sampling N examples in the neighborhood of x :

$$v_{t+1} = \frac{1}{N} \sum_{i=1}^N \nabla_x L_{WACE}(x_{ti}^{adv}, y_o; \theta_h, \mathbf{Z}_h, \bar{n}) - \nabla_x L_{WACE}(x_t^{adv}, y_o; \theta_h, \mathbf{Z}_h, \bar{n})$$

 Update x_{t+1}^{adv} by applying the sign of gradient $x_{t+1}^{adv} = \text{Clip}_x^\epsilon \{x_t^{adv} + \alpha \cdot \text{sign}(g_{t+1})\}$

end for

$$x^{adv} = x_T^{adv}$$

return x^{adv}

Definition 1 (Gradient angle between the surrogate model and the victim model) For the t -th iteration adversarial example x_t^{adv} of the surrogate model f , the angle between $\nabla_x L(x_t^{adv}, y_o; \theta_f)$ and $\nabla_x L(x_t^{adv}, y_o; \theta_h)$ is the gradient angle between f and h at iteration t .

Proposition 1 The better the transferability of the transfer black-box attack, the smaller the gradient angle between the surrogate model and the victim model.

Definition 2 (Top- n wrong categories and top- n wrong categories attack success rate (ASR)) For the example (x, y_o) , if the output of the victim model h is $h(x)$, the top- n wrong categories are \bar{n} number of categories with the largest value in $h(x)$ except the ground truth y_o , which is denoted as $\{y_{\tau_i} \mid i \leq \bar{n}\}$. The top- n wrong categories ASR denotes the accuracy of the adversarial example x^{adv} classified as the wrong category in the top- n wrong categories.

Proposition 2 When the victim model h is attacked by the white-box gradient-based attacks, the successful attacked adversarial examples prefer to be classified as the wrong categories with higher probability (i.e. the top- n wrong categories $\{y_{\tau_i} \mid i \leq \bar{n}\}$). Meanwhile, the higher the probability of the wrong category, the more likely the adversarial example is to be classified as this category.

Therefore, according to Propositions 1 and 2 (the details in Appendix A.3), for the untargeted attack, the weighted augmented CE (WACE) loss is proposed to enhance the transferability of the adversarial examples. Besides maximizing the loss function $L_{CE}(x^{adv}, y_o; \theta_f)$, the WACE loss also minimizes

the loss function $L_{CE}(x^{adv}, y_{\tau_i}; \theta_f)$ where y_{τ_i} belongs to the top- \bar{n} wrong categories $\{y_{\tau_i} | i \leq \bar{n}\}$:

$$L_{WACE}(x, y_o; \theta_f, \mathbf{Z}_h, \bar{n}) = L_{CE}(x, y_o; \theta_f) - \frac{1}{\bar{n}} \sum_{i=1}^{\bar{n}} w_i \cdot L_{CE}(x, y_{\tau_i}; \theta_f) \quad (9)$$

$$w_i = \frac{e^{z_{\tau_i}}}{\sum_{j=1}^{\bar{n}} e^{z_{\tau_j}}} \quad (10)$$

where $\mathbf{Z}_h = h(x) = [z_1, z_2, \dots, z_C]$ is the query logit output of the victim model h to x , \bar{n} is the number of the top- \bar{n} wrong categories. Note that $\sum_{i=1}^{\bar{n}} w_i = 1$, and the higher the logit value of the wrong category, the larger the weight w_i .

According to Proposition 1, the following Theorem 1 verified that the transferability of the transfer black-box attack based on the WACE loss is better than that based on the RCE and CE losses. Theorem 1 is proved in Appendix A.4.

Theorem 1 *The angle between $\nabla_x L_{WACE}(x_t^{adv}, y_o; \theta_f, \mathbf{Z}_h, \bar{n})$ and $\nabla_x L_{CE}(x_t^{adv}, y_o; \theta_h)$ is less than the angle between $\nabla_x L_{RCE}(x_t^{adv}, y_o; \theta_f)$ and $\nabla_x L_{CE}(x_t^{adv}, y_o; \theta_h)$, and the angle between $\nabla_x L_{CE}(x_t^{adv}, y_o; \theta_f)$ and $\nabla_x L_{CE}(x_t^{adv}, y_o; \theta_h)$.*

Propositions 1 and 2 and Theorem 1 are the theoretical analysis of the WACE loss, which explained the high transferability of the WACE loss-based attacks.

3.3 Query prior-based attacks

The family of fast gradient sign methods in Section 2.1 uses the CE loss. However, on the premise of allowing a few queries, the CE loss is replaced by the WACE loss in the family of fast gradient sign methods. Therefore, VMI-FGSM [32] is transformed into query prior-based VMI-FGSM, namely QVMI-FGSM, which is described in Algorithm 1 in detail. Specifically, two changes are made, compared with VMI-FGSM algorithm. First, the CE loss is replaced by our WACE loss. Second, according to Eq. 8, if the maximum number of queries Q is greater than or equal to the number of attack iteration T , QVMI-FGSM queries the logit output of the victim model at each iteration, otherwise, QVMI-FGSM starts from 0 and performs equidistant query with $\lfloor \frac{T}{Q} \rfloor$ as the interval.

Similarly, FGSM [7], I-FGSM [18], MI-FGSM [4], DI-FGSM [39] and SI-NI-FGSM [22] are transformed into Q-FGSM, QI-FGSM, QMI-FGSM, QDI-FGSM and QSI-NI-FGSM by combining the query priors.

4 Experiments

To validate the effectiveness of the proposed query prior-based attacks, we conduct extensive experiments on CIFAR10/100 [17] and ImageNet [26]. In this section, we first introduce the experimental setup, then we compare our method with competitive baselines under various experimental settings. Experimental results demonstrate that our method can significantly improve the transferability of the baselines. Finally, we provide further investigation on hyper-parameters \bar{n} and Q used for query prior-based attacks. Note that the experiments in this section are conducted on VGG16 [28] as the surrogate model for CIFAR10/100 and ResNet50 [10] as the surrogate model for ImageNet with the attack strength $\epsilon = 8/255$. The additional experiments show in Appendix B by using the other surrogate models or increasing the attack strength (i.e. $\epsilon = 16/255$) on CIFAR10/100 and ImageNet. All experiments are run on a single machine with four GeForce RTX 2080tis using Pytorch.

4.1 Experimental setup

Datasets. Different methods are compared on CIFAR10/100 [17] and ImageNet [26]. We randomly pick 2,000 clean images from the CIFAR10/100 test dataset and 1,000 clean images from the ILSVRC 2012 validation set [26], where the selected images are correctly classified by both surrogate model and victim model.

Models. We consider nine naturally trained networks, including VGG16 (V16) [28], VGG19 (V19) [28], ResNet50 (R50) [10], ResNet152 (R152) [10], ResNext50 (RN50) [40], WideResNet-16-4 (WRN-16-4) [43], Inception-v3 (I-v3) [29], DenseNet121 (D121) [11] and MobileNet-v2 (M-v2)

Table 1: The attack success rates (%) on six naturally trained models for CIFAR10 using various transfer attacks and two query attacks with the attack strength $\epsilon = 8/255$. The adversarial examples are generated by VGG16. * denotes the attack success rates under white-box attacks. **Average** means to calculate the average value except *. Note that $Q = 1$ in Q-FGSM.

Model	Attack	Loss	V16	V19	R50	WRN-16-4	D121	M-v2	Average	
VGG16	Square ($Q = 10$)	-	12.65	13.00	14.15	18.75	19.40	27.15	17.52	
	PRGF ($Q = 10$)	-	23.75*	4.30	4.20	5.00	5.20	4.90	4.72	
	FGSM	CE	62.40*	45.20	41.90	46.90	43.55	48.40	45.19	
		RCE	56.65*	41.30	38.45	42.95	39.00	44.25	41.19	
	Q-FGSM (Ours)	WACE	72.85*	49.30	45.50	51.60	47.05	54.65	49.62	
		CE	97.80*	68.95	61.45	72.65	68.30	70.90	68.45	
	I-FGSM	RCE	96.80*	68.10	60.80	72.20	68.10	70.65	67.97	
		WACE	98.80*	74.35	68.65	80.90	76.50	80.35	76.15	
	QI-FGSM (Ours)	CE	93.35*	75.75	70.75	76.05	74.00	74.10	74.13	
		RCE	90.70*	72.60	68.85	72.90	71.40	72.55	71.66	
	MI-FGSM	WACE	96.65*	80.80	77.65	84.20	80.95	84.70	81.66	
		CE	91.30*	69.30	62.80	71.50	69.20	70.60	68.68	
	DI-FGSM	RCE	89.60*	67.20	61.25	68.90	64.90	68.10	66.07	
		WACE	95.85*	74.25	71.15	81.40	76.45	80.80	76.81	
	QDI-FGSM (Ours)	CE	94.00*	72.10	68.10	77.90	72.85	75.55	73.3	
		RCE	98.60*	85.60	80.30	87.45	85.45	86.35	85.03	
	SI-NI-FGSM	WACE	99.25*	88.25	84.95	90.80	89.20	90.70	88.78	
		CE	94.90*	80.00	76.60	81.60	78.40	79.95	79.71	
	VMI-FGSM	RCE	91.70*	77.30	75.50	79.10	76.65	78.75	77.46	
		WACE	97.10*	84.40	83.35	88.40	85.70	89.10	86.19	

[27] and two adversarially trained models, namely adversarial Inception-v3 (a-I-v3) and adversarial ensemble Inception-Resnet-v2 (ae-IR-v2) [31]. We choose VGG16 and ResNet50 as source models for CIFAR10/100 and ImageNet, respectively. The CIFAR10/100 models are trained from scratch and the ImageNet models are the pretrained models in [35, 12].

Baselines. Several most recently proposed methods aiming at generating transferable adversarial examples are taken as baselines, i.e. FGSM [7], I-FGSM [18], MI-FGSM [4], DI-FGSM [39], SI-NI-FGSM [22] and VMI-FGSM [32]. In addition, the RCE loss [44], which is integrated into the above transfer attacks instead of cross-entropy loss (CE), and two black-box query attacks, i.e. P-RGF [3] and Square [1], are taken as baselines to further validate the effectiveness of our method.

Hyper-parameters. On CIFAR10/100 and ImageNet, we set the maximum perturbation, number of iteration and step size as $\epsilon, T, \alpha = 8/255, 10, 0.8/255$ or $16/255, 10, 1.6/255$. We set the decay factor $\mu = 1.0$ for MI-FGSM, SI-NI-FGSM and VMI-FGSM. The transformation probability is set to 0.5 for DI-FGSM. The number of scale copies is 5 for SI-NI-FGSM. The number of sampled examples in the neighborhood and the upper bound of neighborhood are 20 and 1.5, respectively. The number of query, which is the same as that of our query prior-based attacks, is set to $Q = 10$ for Square and P-RGF. For the proposed method, we set $\bar{n}=1$ and $Q = 10$ for CIFAR10, $\bar{n}=5$ and $Q = 10$ for CIFAR100 and ImageNet.

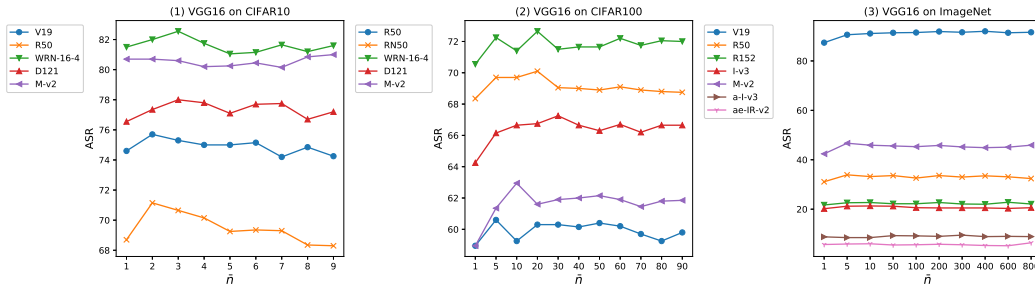


Figure 1: The attack success rates (%) on the victim models with adversarial examples generated by QI-FGSM ($\epsilon = 8/255$) for CIFAR10/100 and ImageNet (the surrogate model is VGG16) when varying the number of the top- \bar{n} wrong categories \bar{n} .

Table 2: The attack success rates (%) on six naturally trained models for CIFAR100 using various transfer attacks and two query attacks with the attack strength $\epsilon = 8/255$. The adversarial examples are generated by VGG16. * denotes the attack success rates under white-box attacks. **Average** means to calculate the average value except *. Note that $Q = 1$ in Q-FGSM.

Model	Attack	Loss	V16	R50	RN50	WRN-16-4	D121	M-v2	Average	
VGG16	Square ($Q = 10$)	-	36.75	31.60	39.40	41.40	33.40	49.90	38.74	
	PRGF ($Q = 10$)	-	46.20*	6.90	8.10	8.00	6.95	6.95	7.38	
	FGSM	CE	85.75*	63.15	64.30	68.65	66.25	66.45	65.76	
		RCE	83.55*	61.05	63.25	67.20	65.25	64.40	64.23	
	Q-FGSM (Ours)	WACE	85.30*	63.20	65.65	68.75	67.00	67.65	66.45	66.45
		CE	99.60*	50.70	58.70	61.15	54.10	50.65	55.06	
	I-FGSM	RCE	99.50*	47.25	56.30	60.00	54.10	52.90	54.11	
		WACE	99.75*	60.70	69.45	72.05	66.70	61.50	66.08	
	QI-FGSM (Ours)	CE	99.30*	69.30	72.75	76.35	71.10	69.35	71.77	
		RCE	99.10*	68.20	72.50	76.05	72.55	70.25	71.91	
	MI-FGSM	WACE	99.30*	76.50	79.80	82.50	77.70	76.45	78.59	
		CE	98.60*	59.30	64.05	66.35	60.25	58.50	61.69	
	DI-FGSM	RCE	97.30*	57.60	63.90	67.70	59.70	62.25	62.23	
		WACE	99.00*	67.05	73.45	75.60	69.45	69.40	70.99	
	QDI-FGSM (Ours)	CE	96.75*	64.35	70.10	73.90	70.65	68.20	69.44	
		RCE	99.60*	71.65	76.15	80.05	76.10	75.25	75.84	
	QSI-FGSM (Ours)	WACE	99.90*	77.15	81.40	83.70	80.55	77.75	80.11	
		CE	99.55*	77.70	80.00	82.85	79.70	76.85	79.42	
	VMI-FGSM	RCE	99.05*	79.20	80.20	83.90	80.30	79.65	80.65	
		WACE	99.35*	83.30	85.50	87.75	84.40	81.40	84.47	

Table 3: The attack success rates (%) of six naturally trained models and two adversarially trained models on ImageNet using various transfer attacks and two query attacks with the attack strength $\epsilon = 8/255$. The adversarial examples are generated on ResNet50. * denotes the attack success rates under white-box attacks. **Avg.** means to calculate the average value of the naturally trained models except *. Note that $Q = 1$ in Q-FGSM.

Model	Attack	Loss	V16	V19	R50	R152	I-v3	M-v2	Avg.	a-I-v3	ae-IR-v2
ResNet50	Square ($Q = 0$)	-	37.5	35.3	18.1	12.9	18.2	35.8	26.3	13.8	13.4
	Square ($Q = 1$)	-	38.8	36.5	20.2	14.6	19.1	37.4	27.8	16.3	14.8
	Square ($Q = 10$)	-	44.4	41.4	25.6	18.3	24.1	43.7	32.9	21.7	17.6
	PRGF ($Q = 10$)	-	6.9	5.5	80.2*	-	3.2	7.1	5.7	3.2	1.7
	FGSM	CE	42.6	40.8	90.4*	42.3	29.9	41.2	39.4	20.5	11.5
		RCE	37.7	36.2	80.5*	30.6	24.6	35.2	32.9	19.0	10.2
	Q-FGSM (Ours)	WACE	44.2	42.5	90.7*	42.6	31.2	42.8	40.7	20.1	10.8
		CE	32.1	29.7	100*	45.0	17.0	33.2	31.4	9.1	6.0
	I-FGSM	RCE	28.9	28.0	100*	35.2	16.2	29.7	27.6	8.4	5.7
		WACE	39.9	36.6	100*	53.0	22.6	44.4	39.3	10.9	7.3
	QI-FGSM (Ours)	CE	55.4	53.0	100*	70.7	37.8	58.6	55.1	17.1	11.9
		RCE	57.1	56.6	100*	63.6	35.9	56.2	53.9	16.1	11.6
	MI-FGSM	WACE	62.5	60.5	100*	74.8	43.1	65.0	61.2	19.9	13.3
		CE	52.6	49.2	100*	62.7	36.9	56.0	51.5	11.7	9.3
	DI-FGSM	RCE	46.1	46.9	100*	53.0	36.1	48.4	46.1	12.2	9.5
		WACE	61.0	56.9	100*	68.9	41.5	64.5	58.6	16.9	12.7
	QDI-FGSM (Ours)	CE	68.7	68.2	100*	81.8	51.4	72.3	68.5	24.2	16.7
		RCE	70.5	69.5	100*	81.0	52.5	73.7	69.4	21.6	16.1
	QSI-FGSM (Ours)	WACE	73.1	72.0	100*	87.1	57.0	78.9	73.6	26.1	21.0
		CE	69.1	68.5	99.9*	83.9	53.1	72.1	69.3	21.4	16.9
	VMI-FGSM	RCE	69.9	70.9	100*	79.5	52.1	71.8	68.8	22.1	18.7
		WACE	78.6	74.8	100*	88.2	60.8	82.3	76.9	27.3	23.2

4.2 Comparison with or without the query priors

Attacking a naturally trained model. To validate that the query priors can enhance the transferability of the transfer attacks, we perform six transfer attacks with or without the query priors to attack six naturally trained models for CIFAR10/100 and ImageNet. As shown in Tables 1, 2 and 3, when the attack strength $\epsilon = 8/255$, the query prior-based attacks can not only significantly improve the transfer attack success rate of the black-box setting but also improve the attack success rate of the white-box setting. The average increase of the ASR is 4.43% on Q-FGSM and 6.88 to 15.48% on the other five transfer attacks for CIFAR10, 0.69% on Q-FGSM and 5.05 to 11.02% on the other five transfer attacks for CIFAR100, 1.3% on Q-FGSM and 5.1 to 7.9% on the other five transfer attacks for ImageNet.

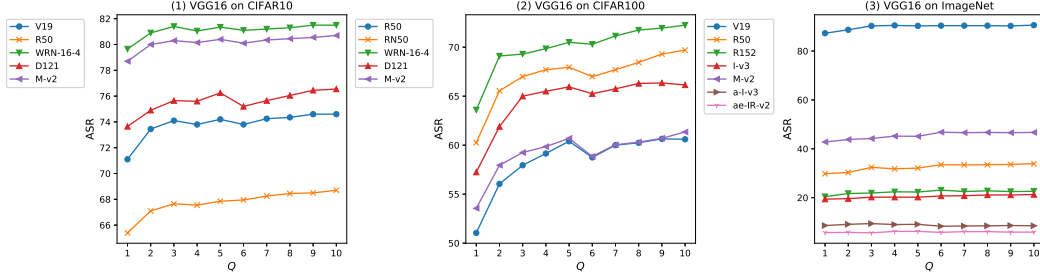


Figure 2: The attack success rates (%) on the victim models with adversarial examples generated by QI-FGSM ($\epsilon = 8/255$) for CIFAR10/100 and ImageNet (the surrogate model is VGG16) when varying the number of queries Q .

Attacking an adversarially trained model. Table 3 performs six transfer attacks with or without the query priors to attack two adversarially trained models for ImageNet. The results show that the query prior-based attacks can enhance the transferability of gradient iterative-based attacks when attacking the adversarially trained model. Except for a slight decrease on Q-FGSM, the increase of the ASR is 1.3 to 6.3% on the other five transfer attacks for ImageNet.

4.3 Comparison between different loss functions

Attacking a naturally trained model. RCE loss [44] is a new normalized CE loss to escape from the poor local maxima for enhancing the transferability of adversarial examples. To verify that the transferability of the query prior-based attacks is better than the RCE loss based attacks, we perform six transfer attacks with or without the query priors to attack six naturally trained models for CIFAR10/100 and ImageNet. As shown in Table 1, 2 and 3, when the attack strength $\epsilon = 8/255$, in comparison with the RCE loss based attacks, the query prior-based attacks can not only significantly improve the transfer attack success rate of the black-box setting, but also improve the attack success rate of the white-box setting. The average increase of the ASR is 8.43% on Q-FGSM and 3.75 to 10.75% on the other five transfer attacks for CIFAR10, 2.22% on Q-FGSM and 3.82 to 11.97% on the other five transfer attacks for CIFAR100, 7.8% on Q-FGSM and 4.2 to 12.5% on the other five transfer attacks for ImageNet.

Attacking an adversarially trained model. Table 3 performs six query prior-based transfer attacks and six RCE loss-based transfer attacks to attack two adversarially trained models for ImageNet. In comparison with the RCE loss-based attacks, the query prior-based attacks can enhance the transferability of adversarial examples when attacking the adversarially trained model. The increase of the ASR is 0.6 to 1.1% on Q-FGSM and 1.6 to 5.2% on the other five transfer attacks for ImageNet.

4.4 Comparison with current black-box query attacks

Black-box query attacks. Square [1] is a very effective score-based query attack, and its performance sometimes even exceeds that of the white-box attacks. Tables 1, 2 and 3 evaluate that the attack success rates of the query prior-based attacks are much higher than that of Square with the same few queries for CIFAR10/100 and ImageNet when these attack methods attack six naturally trained models. By comparing the best query prior-based attacks with Square, the average increase of the ASR is 71.26% for CIFAR10, 45.73% for CIFAR100 and 44% for ImageNet. When these attack methods attack two adversarially trained models, some query prior-based attacks are better than Square with the same few queries for ImageNet. By comparing the best query prior-based attacks with Square, the increase is 5.6% on both adversarially trained models.

Transferable prior-based black-box query attacks. P-RGF [3] is an effective transferable prior-based query attack, which can significantly decrease the query number. Table 1, 2 and 3 show that P-RGF is inefficient at limits of few queries on six naturally trained models and two adversarially trained models for CIFAR10/100 and ImageNet. By comparing the best query prior-based attacks with P-RGF on six naturally trained models, the average increase of the ASR is 84.06% for CIFAR10, 77.09% for CIFAR100 and 71.2% for ImageNet. On two adversarially trained models, the increase of the ASR is 24.1% and 21.5% for ImageNet, respectively.

4.5 Ablation study on Hyper-parameters

Different numbers of top-n wrong categories. Figure 1 evaluates the effect of different \bar{n} on the attack success rates of five naturally trained victim models and two adversarially trained victim models when these victim models are attacked by QI-FGSM ($\epsilon = 8/255$) with VGG16 for CIFAR10/100 and ImageNet. When \bar{n} is greater than a certain threshold, the attack success rate will not be improved, e.g. the threshold is 2 for CIFAR10, 10 for CIFAR100 and 5 for ImageNet approximately. Because increasing \bar{n} increases the calculation time of the gradient, \bar{n} is not the bigger the better.

Different query numbers. Figure 2 evaluates the effect of different Q on the attack success rates of five naturally trained victim models and two adversarially trained victim models when these victim models are attacked by QI-FGSM ($\epsilon = 8/255$) with VGG16 for CIFAR10/100 and ImageNet. On the victim models, the more the query, the greater the attack success rate. When the query number increases from 1 to 10, the attack success rate increases by 3.5% at most for CIFAR10, 10% at most for CIFAR100 and 5% at most for ImageNet approximately, and the increased attack success rate is mainly increased in the first five queries.

4.6 Limitation

The query prior-based attacks are effective for the untargeted attack. However, because Proposition 2 is more conducive to the exploration of the untargeted attack than the targeted attack, the proposed query prior-based attacks are designed as the untargeted attacks, which may not work in the targeted attack. In the future, the design of the query prior-based targeted attack is still a problem that needs to be studied.

5 Related Work

5.1 Adversarial Attacks

Black-box Transfer Attacks are divided into five categories, i.e. feature destruction-based attacks, gradient generation-based attacks, data augmentation-based attacks, model ensemble-based attacks, model specific-based attacks, respectively. The feature destruction-based attacks [38, 16, 15, 13, 46, 48, 5, 34] enhance the transferability of adversarial examples by destroying the features of the intermediate layers or critical neurons. The gradient generation-based attacks [19, 8, 39, 6, 22, 4, 9, 32] enhance the transferability of adversarial examples by changing the way of gradient generation. The data augmentation-based attacks [33, 20, 49, 14] increase the input diversity to enhance the transferability of adversarial examples. The model ensemble-based attacks [23, 21, 41] use the common attention of various models to enhance the transferability of adversarial examples. The model specific-based attacks [37] use the high transferability of some structures to enhance the transferability of adversarial examples, e.g. skip connection.

Black-box Query Attacks are divided into two categories, i.e., pure query attacks and transferable prior-based query attacks. The pure query attacks [2, 1, 47] estimate the gradient or update the attack optimization model by querying the output of the victim model. Recently, Zhang et al. [47] utilized the feedback knowledge not only to craft adversarial examples but also to alter the searching directions to achieve efficient attacks. The transferable prior-based query attacks [3, 42, 30] use the prior knowledge of the surrogate model to decrease the query number. Recently, Tashiro et al. [30] proposed Output Diversified Sampling to maximize diversity in the target model’s outputs among the generated samples.

5.2 Adversarial Defenses

Adversarial training [24, 45, 36, 25] is the most effective method to defend against adversarial examples. Recently, Zhang et al. [45] designed a new defense method to trade off the adversarial robustness against accuracy. Wong et al. [36] discovered that adversarial training can use a much weaker and cheaper adversary, an approach that was previously believed to be ineffective, rendering the method no more costly than standard training in practice. Pang et al. [25] investigated the effects of mostly overlooked training tricks and hyperparameters for the adversarially trained models.

6 Conclusion

Though transferable priors decrease the query number of the black-box query attacks, the average number of queries is still larger than 100, which is easily affected by the number of queries limit policy. On the contrary, we can utilize the priors of a few queries to enhance the transferability of the transfer attacks. In this work, we propose the query prior-based method to enhance the transferability of the family of FGSMs. Specifically, we find that: (i) The better the transferability of the transfer attack, the smaller the gradient angle between the surrogate model and the victim model. (ii) The successful attacked adversarial examples prefer to be classified as the wrong categories with higher probability by the victim model. Based on the above findings, the weighted augmented cross-entropy (WACE) loss is proposed to decrease the gradient angle between the surrogate model and the victim model for enhancing the transferability of adversarial examples. Theoretical analysis and extensive experiments demonstrate the effectiveness of the query prior-based attacks.

References

- [1] Maksym Andriushchenko, Francesco Croce, Nicolas Flammarion, and Matthias Hein. Square attack: A query-efficient black-box adversarial attack via random search. In *Computer Vision - ECCV 2020 - 16th European Conference, Glasgow, UK, August 23-28, 2020, Proceedings, Part XXIII*, volume 12368 of *Lecture Notes in Computer Science*, pages 484–501. Springer, 2020.
- [2] Pin-Yu Chen, Huan Zhang, Yash Sharma, Jinfeng Yi, and Cho-Jui Hsieh. ZOO: zeroth order optimization based black-box attacks to deep neural networks without training substitute models. In *Proceedings of the 10th ACM Workshop on Artificial Intelligence and Security, AISec@CCS 2017, Dallas, TX, USA, November 3, 2017*, pages 15–26. ACM, 2017.
- [3] Shuyu Cheng, Yinpeng Dong, Tianyu Pang, Hang Su, and Jun Zhu. Improving black-box adversarial attacks with a transfer-based prior. In *Advances in Neural Information Processing Systems 32: Annual Conference on Neural Information Processing Systems 2019, NeurIPS 2019, December 8-14, 2019, Vancouver, BC, Canada*, pages 10932–10942, 2019.
- [4] Yinpeng Dong, Fangzhou Liao, Tianyu Pang, Hang Su, Jun Zhu, Xiaolin Hu, and Jianguo Li. Boosting adversarial attacks with momentum. In *2018 IEEE Conference on Computer Vision and Pattern Recognition, CVPR 2018, Salt Lake City, UT, USA, June 18-22, 2018*, pages 9185–9193. Computer Vision Foundation / IEEE Computer Society, 2018.
- [5] Aditya Ganeshan, Vivek B. S., and Venkatesh Babu Radhakrishnan. FDA: feature disruptive attack. In *2019 IEEE/CVF International Conference on Computer Vision, ICCV 2019, Seoul, Korea (South), October 27 - November 2, 2019*, pages 8068–8078. IEEE, 2019.
- [6] Lianli Gao, Qilong Zhang, Jingkuan Song, Xianglong Liu, and Heng Tao Shen. Patch-wise attack for fooling deep neural network. In *Computer Vision - ECCV 2020 - 16th European Conference, Glasgow, UK, August 23-28, 2020, Proceedings, Part XXVIII*, volume 12373 of *Lecture Notes in Computer Science*, pages 307–322. Springer, 2020.
- [7] Ian J. Goodfellow, Jonathon Shlens, and Christian Szegedy. Explaining and harnessing adversarial examples. In *3rd International Conference on Learning Representations, ICLR 2015, San Diego, CA, USA, May 7-9, 2015, Conference Track Proceedings*, 2015.
- [8] Yiwen Guo, Qizhang Li, and Hao Chen. Backpropagating linearly improves transferability of adversarial examples. In *Advances in Neural Information Processing Systems 33: Annual Conference on Neural Information Processing Systems 2020, NeurIPS 2020, December 6-12, 2020, virtual*, 2020.
- [9] Xu Han, Anmin Liu, Yifeng Xiong, Yanbo Fan, and Kun He. Sampling-based fast gradient rescaling method for highly transferable adversarial attacks. *CoRR*, abs/2204.02887, 2022.
- [10] Kaiming He, Xiangyu Zhang, Shaoqing Ren, and Jian Sun. Deep residual learning for image recognition. In *2016 IEEE Conference on Computer Vision and Pattern Recognition, CVPR 2016, Las Vegas, NV, USA, June 27-30, 2016*, pages 770–778. IEEE Computer Society, 2016.
- [11] Gao Huang, Zhuang Liu, Laurens van der Maaten, and Kilian Q. Weinberger. Densely connected convolutional networks. In *2017 IEEE Conference on Computer Vision and Pattern Recognition, CVPR 2017, Honolulu, HI, USA, July 21-26, 2017*, pages 2261–2269. IEEE Computer Society, 2017.

- [12] Howard Huang. torchvision.models. <https://pytorch.org/vision/stable/models.html>, 2017.
- [13] Qian Huang, Isay Katsman, Zeqi Gu, Horace He, Serge J. Belongie, and Ser-Nam Lim. Enhancing adversarial example transferability with an intermediate level attack. In *2019 IEEE/CVF International Conference on Computer Vision, ICCV 2019, Seoul, Korea (South), October 27 - November 2, 2019*, pages 4732–4741. IEEE, 2019.
- [14] Tianjin Huang, Vlado Menkovski, Yulong Pei, Yuhao Wang, and Mykola Pechenizkiy. Direction-aggregated attack for transferable adversarial examples. *CoRR*, abs/2104.09172, 2021.
- [15] Nathan Inkawhich, Kevin J. Liang, Binghui Wang, Matthew Inkawhich, Lawrence Carin, and Yiran Chen. Perturbing across the feature hierarchy to improve standard and strict blackbox attack transferability. In *Advances in Neural Information Processing Systems 33: Annual Conference on Neural Information Processing Systems 2020, NeurIPS 2020, December 6-12, 2020, virtual*, 2020.
- [16] Nathan Inkawhich, Wei Wen, Hai (Helen) Li, and Yiran Chen. Feature space perturbations yield more transferable adversarial examples. In *IEEE Conference on Computer Vision and Pattern Recognition, CVPR 2019, Long Beach, CA, USA, June 16-20, 2019*, pages 7066–7074. Computer Vision Foundation / IEEE, 2019.
- [17] Alex Krizhevsky. Learning multiple layers of features from tiny images. 2009.
- [18] Alexey Kurakin, Ian J. Goodfellow, and Samy Bengio. Adversarial examples in the physical world. In *5th International Conference on Learning Representations, ICLR 2017, Toulon, France, April 24-26, 2017, Workshop Track Proceedings*. OpenReview.net, 2017.
- [19] Qizhang Li, Yiwen Guo, and Hao Chen. Yet another intermediate-level attack. In *Computer Vision - ECCV 2020 - 16th European Conference, Glasgow, UK, August 23-28, 2020, Proceedings, Part XVI*, volume 12361 of *Lecture Notes in Computer Science*, pages 241–257. Springer, 2020.
- [20] Yingwei Li, Song Bai, Cihang Xie, Zhenyu Liao, Xiaohui Shen, and Alan L. Yuille. Regional homogeneity: Towards learning transferable universal adversarial perturbations against defenses. In *Computer Vision - ECCV 2020 - 16th European Conference, Glasgow, UK, August 23-28, 2020, Proceedings, Part XI*, volume 12356 of *Lecture Notes in Computer Science*, pages 795–813. Springer, 2020.
- [21] Yingwei Li, Song Bai, Yuyin Zhou, Cihang Xie, Zhishuai Zhang, and Alan L. Yuille. Learning transferable adversarial examples via ghost networks. In *The Thirty-Fourth AAAI Conference on Artificial Intelligence, AAAI 2020, The Thirty-Second Innovative Applications of Artificial Intelligence Conference, IAAI 2020, The Tenth AAAI Symposium on Educational Advances in Artificial Intelligence, EAAI 2020, New York, NY, USA, February 7-12, 2020*, pages 11458–11465. AAAI Press, 2020.
- [22] Jiadong Lin, Chuanbiao Song, Kun He, Liwei Wang, and John E. Hopcroft. Nesterov accelerated gradient and scale invariance for adversarial attacks. In *8th International Conference on Learning Representations, ICLR 2020, Addis Ababa, Ethiopia, April 26-30, 2020*. OpenReview.net, 2020.
- [23] Yanpei Liu, Xinyun Chen, Chang Liu, and Dawn Song. Delving into transferable adversarial examples and black-box attacks. In *5th International Conference on Learning Representations, ICLR 2017, Toulon, France, April 24-26, 2017, Conference Track Proceedings*. OpenReview.net, 2017.
- [24] Aleksander Madry, Aleksandar Makelov, Ludwig Schmidt, Dimitris Tsipras, and Adrian Vladu. Towards deep learning models resistant to adversarial attacks. In *6th International Conference on Learning Representations, ICLR 2018, Vancouver, BC, Canada, April 30 - May 3, 2018, Conference Track Proceedings*. OpenReview.net, 2018.
- [25] Tianyu Pang, Xiao Yang, Yinpeng Dong, Hang Su, and Jun Zhu. Bag of tricks for adversarial training. In *9th International Conference on Learning Representations, ICLR 2021, Virtual Event, Austria, May 3-7, 2021*. OpenReview.net, 2021.
- [26] Olga Russakovsky, Jia Deng, Hao Su, Jonathan Krause, Sanjeev Satheesh, Sean Ma, Zhiheng Huang, Andrej Karpathy, Aditya Khosla, Michael S. Bernstein, Alexander C. Berg, and Li Fei-Fei. Imagenet large scale visual recognition challenge. *Int. J. Comput. Vis.*, 115(3):211–252, 2015.

- [27] Mark Sandler, Andrew G. Howard, Menglong Zhu, Andrey Zhmoginov, and Liang-Chieh Chen. Mobilenetv2: Inverted residuals and linear bottlenecks. In *2018 IEEE Conference on Computer Vision and Pattern Recognition, CVPR 2018, Salt Lake City, UT, USA, June 18-22, 2018*, pages 4510–4520. Computer Vision Foundation / IEEE Computer Society, 2018.
- [28] Karen Simonyan and Andrew Zisserman. Very deep convolutional networks for large-scale image recognition. In *3rd International Conference on Learning Representations, ICLR 2015, San Diego, CA, USA, May 7-9, 2015, Conference Track Proceedings*, 2015.
- [29] Christian Szegedy, Vincent Vanhoucke, Sergey Ioffe, Jonathon Shlens, and Zbigniew Wojna. Rethinking the inception architecture for computer vision. In *2016 IEEE Conference on Computer Vision and Pattern Recognition, CVPR 2016, Las Vegas, NV, USA, June 27-30, 2016*, pages 2818–2826. IEEE Computer Society, 2016.
- [30] Yusuke Tashiro, Yang Song, and Stefano Ermon. Diversity can be transferred: Output diversification for white- and black-box attacks. In *Advances in Neural Information Processing Systems 33: Annual Conference on Neural Information Processing Systems 2020, NeurIPS 2020, December 6-12, 2020, virtual*, 2020.
- [31] Florian Tramèr, Alexey Kurakin, Nicolas Papernot, Ian J. Goodfellow, Dan Boneh, and Patrick D. McDaniel. Ensemble adversarial training: Attacks and defenses. In *6th International Conference on Learning Representations, ICLR 2018, Vancouver, BC, Canada, April 30 - May 3, 2018, Conference Track Proceedings*. OpenReview.net, 2018.
- [32] Xiaosen Wang and Kun He. Enhancing the transferability of adversarial attacks through variance tuning. In *IEEE Conference on Computer Vision and Pattern Recognition, CVPR 2021, virtual, June 19-25, 2021*, pages 1924–1933. Computer Vision Foundation / IEEE, 2021.
- [33] Xiaosen Wang, Xuanran He, Jingdong Wang, and Kun He. Admix: Enhancing the transferability of adversarial attacks. In *2021 IEEE/CVF International Conference on Computer Vision, ICCV 2021, Montreal, QC, Canada, October 10-17, 2021*, pages 16138–16147. IEEE, 2021.
- [34] Zhibo Wang, Hengchang Guo, Zhifei Zhang, Wenxin Liu, Zhan Qin, and Kui Ren. Feature importance-aware transferable adversarial attacks. In *2021 IEEE/CVF International Conference on Computer Vision, ICCV 2021, Montreal, QC, Canada, October 10-17, 2021*, pages 7619–7628. IEEE, 2021.
- [35] Ross Wightman. Pytorch image models. <https://github.com/rwightman/pytorch-image-models>, 2019.
- [36] Eric Wong, Leslie Rice, and J. Zico Kolter. Fast is better than free: Revisiting adversarial training. In *8th International Conference on Learning Representations, ICLR 2020, Addis Ababa, Ethiopia, April 26-30, 2020*. OpenReview.net, 2020.
- [37] Dongxian Wu, Yisen Wang, Shu-Tao Xia, James Bailey, and Xingjun Ma. Skip connections matter: On the transferability of adversarial examples generated with resnets. In *8th International Conference on Learning Representations, ICLR 2020, Addis Ababa, Ethiopia, April 26-30, 2020*. OpenReview.net, 2020.
- [38] Weibin Wu, Yuxin Su, Xixian Chen, Shenglin Zhao, Irwin King, Michael R. Lyu, and Yu-Wing Tai. Boosting the transferability of adversarial samples via attention. In *2020 IEEE/CVF Conference on Computer Vision and Pattern Recognition, CVPR 2020, Seattle, WA, USA, June 13-19, 2020*, pages 1158–1167. Computer Vision Foundation / IEEE, 2020.
- [39] Cihang Xie, Zhishuai Zhang, Yuyin Zhou, Song Bai, Jianyu Wang, Zhou Ren, and Alan L. Yuille. Improving transferability of adversarial examples with input diversity. In *IEEE Conference on Computer Vision and Pattern Recognition, CVPR 2019, Long Beach, CA, USA, June 16-20, 2019*, pages 2730–2739. Computer Vision Foundation / IEEE, 2019.
- [40] Saining Xie, Ross B. Girshick, Piotr Dollár, Zhuowen Tu, and Kaiming He. Aggregated residual transformations for deep neural networks. In *2017 IEEE Conference on Computer Vision and Pattern Recognition, CVPR 2017, Honolulu, HI, USA, July 21-26, 2017*, pages 5987–5995. IEEE Computer Society, 2017.
- [41] Yifeng Xiong, Jiadong Lin, Min Zhang, John E. Hopcroft, and Kun He. Stochastic variance reduced ensemble adversarial attack for boosting the adversarial transferability. *CoRR*, abs/2111.10752, 2021.

- [42] Jiancheng Yang, Yangzhou Jiang, Xiaoyang Huang, Bingbing Ni, and Chenglong Zhao. Learning black-box attackers with transferable priors and query feedback. In *Advances in Neural Information Processing Systems 33: Annual Conference on Neural Information Processing Systems 2020, NeurIPS 2020, December 6-12, 2020, virtual*, 2020.
- [43] Sergey Zagoruyko and Nikos Komodakis. Wide residual networks. In *Proceedings of the British Machine Vision Conference 2016, BMVC 2016, York, UK, September 19-22, 2016*. BMVA Press, 2016.
- [44] Chaoning Zhang, Philipp Benz, Adil Karjauv, Jae-Won Cho, Kang Zhang, and In So Kweon. Investigating top-k white-box and transferable black-box attack. *CoRR*, abs/2204.00089, 2022.
- [45] Hongyang Zhang, Yaodong Yu, Jiantao Jiao, Eric P. Xing, Laurent El Ghaoui, and Michael I. Jordan. Theoretically principled trade-off between robustness and accuracy. In *Proceedings of the 36th International Conference on Machine Learning, ICML 2019, 9-15 June 2019, Long Beach, California, USA*, volume 97 of *Proceedings of Machine Learning Research*, pages 7472–7482. PMLR, 2019.
- [46] Jianping Zhang, Weibin Wu, Jen-tse Huang, Yizhan Huang, Wenxuan Wang, Yuxin Su, and Michael R. Lyu. Improving adversarial transferability via neuron attribution-based attacks. *CoRR*, abs/2204.00008, 2022.
- [47] Yonggang Zhang, Ya Li, Tongliang Liu, and Xinmei Tian. Dual-path distillation: A unified framework to improve black-box attacks. In *Proceedings of the 37th International Conference on Machine Learning, ICML 2020, 13-18 July 2020, Virtual Event*, volume 119 of *Proceedings of Machine Learning Research*, pages 11163–11172. PMLR, 2020.
- [48] Wen Zhou, Xin Hou, Yongjun Chen, Mengyun Tang, Xiangqi Huang, Xiang Gan, and Yong Yang. Transferable adversarial perturbations. In *Computer Vision - ECCV 2018 - 15th European Conference, Munich, Germany, September 8-14, 2018, Proceedings, Part XIV*, volume 11218 of *Lecture Notes in Computer Science*, pages 471–486. Springer, 2018.
- [49] Junhua Zou, Zhisong Pan, Junyang Qiu, Xin Liu, Ting Rui, and Wei Li. Improving the transferability of adversarial examples with resized-diverse-inputs, diversity-ensemble and region fitting. In *Computer Vision - ECCV 2020 - 16th European Conference, Glasgow, UK, August 23-28, 2020, Proceedings, Part XXII*, volume 12367 of *Lecture Notes in Computer Science*, pages 563–579. Springer, 2020.

Checklist

The checklist follows the references. Please read the checklist guidelines carefully for information on how to answer these questions. For each question, change the default **[TODO]** to **[Yes]**, **[No]**, or **[N/A]**. You are strongly encouraged to include a **justification to your answer**, either by referencing the appropriate section of your paper or providing a brief inline description. For example:

- Did you include the license to the code and datasets? **[Yes]** See Section ??.
- Did you include the license to the code and datasets? **[No]** The code and the data are proprietary.
- Did you include the license to the code and datasets? **[N/A]**

Please do not modify the questions and only use the provided macros for your answers. Note that the Checklist section does not count towards the page limit. In your paper, please delete this instructions block and only keep the Checklist section heading above along with the questions/answers below.

1. For all authors...
 - (a) Do the main claims made in the abstract and introduction accurately reflect the paper’s contributions and scope? **[Yes]**
 - (b) Did you describe the limitations of your work? **[Yes]** See Section 4.6
 - (c) Did you discuss any potential negative societal impacts of your work? **[No]**
 - (d) Have you read the ethics review guidelines and ensured that your paper conforms to them? **[Yes]**
2. If you are including theoretical results...

- (a) Did you state the full set of assumptions of all theoretical results? [Yes]
 - (b) Did you include complete proofs of all theoretical results? [Yes] Proposition 1 and 2 and Theorem 1 have been proved.
3. If you ran experiments...
- (a) Did you include the code, data, and instructions needed to reproduce the main experimental results (either in the supplemental material or as a URL)? [Yes]
 - (b) Did you specify all the training details (e.g., data splits, hyperparameters, how they were chosen)? [Yes] See Section 4.1
 - (c) Did you report error bars (e.g., with respect to the random seed after running experiments multiple times)? [No] But we made a lot of experiments on different models and different parameters to verify the effectiveness of the proposed method.
 - (d) Did you include the total amount of compute and the type of resources used (e.g., type of GPUs, internal cluster, or cloud provider)? [Yes]
4. If you are using existing assets (e.g., code, data, models) or curating/releasing new assets...
- (a) If your work uses existing assets, did you cite the creators? [Yes] See Section 4.1
 - (b) Did you mention the license of the assets? [No]
 - (c) Did you include any new assets either in the supplemental material or as a URL? [Yes]
 - (d) Did you discuss whether and how consent was obtained from people whose data you're using/curating? [Yes] We cited the CIFAR10/100 and ImageNet datasets.
 - (e) Did you discuss whether the data you are using/curating contains personally identifiable information or offensive content? [No]
5. If you used crowdsourcing or conducted research with human subjects...
- (a) Did you include the full text of instructions given to participants and screenshots, if applicable? [N/A]
 - (b) Did you describe any potential participant risks, with links to Institutional Review Board (IRB) approvals, if applicable? [N/A]
 - (c) Did you include the estimated hourly wage paid to participants and the total amount spent on participant compensation? [N/A]

A Proofs

We provide the proofs in this section.

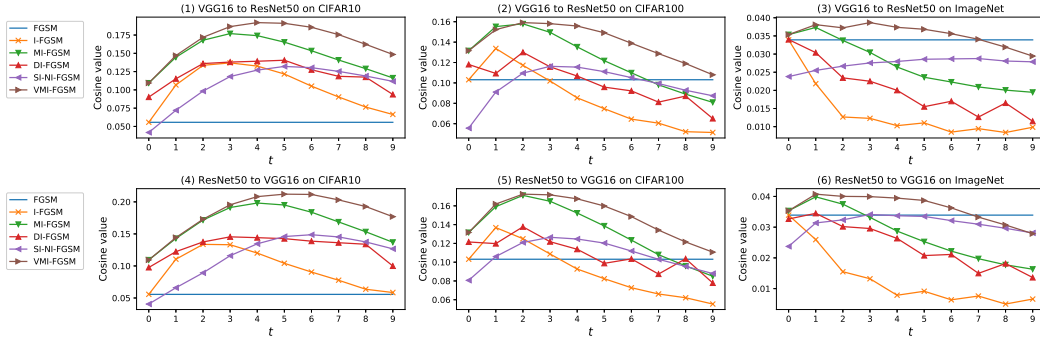


Figure 3: The cosine value of the gradient angle between the surrogate model and the victim model at each iteration when the surrogate model is attacked by different methods for CIFAR10/100 and ImageNet. For example, in subfigure (1), VGG16 as the surrogate model and ResNet50 as the victim model are attacked by different transfer attacks for CIFAR10. Note that the attack strength $\epsilon = 8/255$.

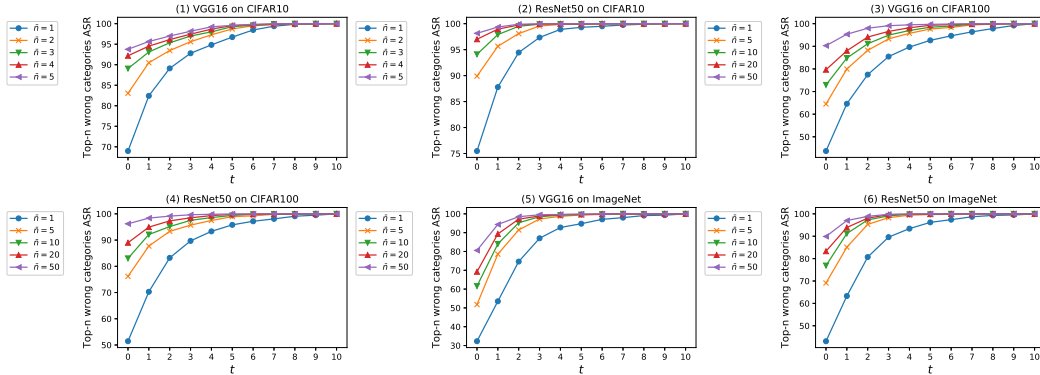


Figure 4: The top-n wrong categories attack success rate (ASR) (%) at each iteration t when the model is attacked by I-FGSM (white-box setting) for CIFAR10/100 and ImageNet. For example, in subfigure (1), VGG16 is attacked by I-FGSM for CIFAR10. The successful attacked adversarial examples prefer to be classified as the top-n wrong categories. With the increase of the iteration, the top-n wrong categories ASR gradually increases and approaches 100%. Note that the attack strength $\epsilon = 8/255$.

A.1 Proof of Proposition 1

Proposition 1: *The better the transferability of the transfer black-box attack, the smaller the gradient angle between the surrogate model and the victim model.*

Proof 1 *To verify the correctness of Proposition 1, we compare between the attack success rates of the family of fast gradient sign methods and the cosine values (i.e., the average cosine values of the gradient angles between the surrogate model and the victim model at all iterations) of the family of fast gradient sign methods where the attack strength, number of iteration and step size are $\epsilon, T, \alpha = 8/255, 10, 0.8/255$. If the sort of the attack success rates is the same as the sort of the cosine values, Proposition 1 is correct with high confidence.*

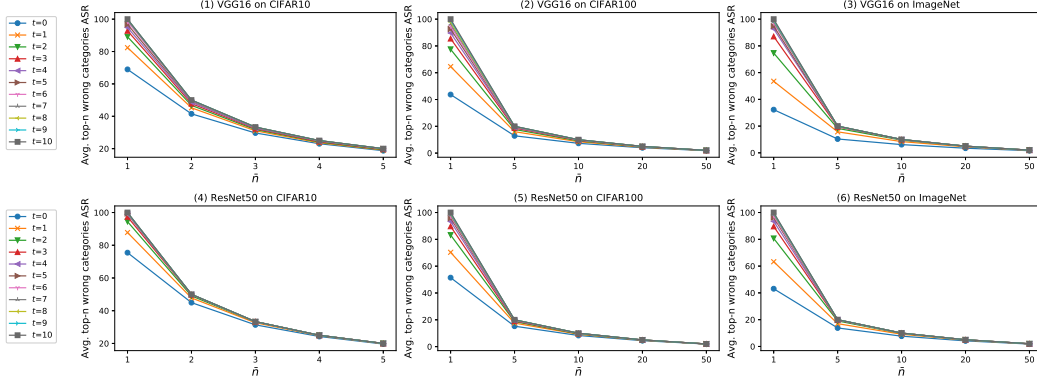


Figure 5: The average top- n wrong categories attack success rate (ASR) (%) at each iteration t when the model is attacked by I-FGSM (white-box setting) for CIFAR10/100 and ImageNet. For example, in subfigure (1), VGG16 is attacked by I-FGSM for CIFAR10. The smaller \bar{n} , the higher the average top- n wrong categories ASR. Therefore, the higher the probability of the wrong category, the more likely the adversarial example is to be classified as this category. Note that the attack strength $\epsilon = 8/255$.

When VGG16 is the surrogate model and ResNet50 is the victim model for CIFAR10, the sort of the attack success rates is VMI-FGSM (76.60%) > MI-FGSM (70.75%) > SI-NI-FGSM (68.10%) > DI-FGSM (62.80%) > I-FGSM (61.45%) > FGSM (41.90%), and the Figure 3-(1) shows that the sort of the cosine values is also basically VMI-FGSM > MI-FGSM > SI-NI-FGSM > DI-FGSM > I-FGSM > FGSM.

When VGG16 is the surrogate model and ResNet50 is the victim model for CIFAR100, the sort of the attack success rates is VMI-FGSM (80.00%) > MI-FGSM (72.75%) > SI-NI-FGSM (70.10%) > FGSM (64.30%) \approx DI-FGSM (64.05%) > I-FGSM (58.70%), and the Figure 3-(2) shows that the sort of the cosine values is also basically VMI-FGSM > MI-FGSM > SI-NI-FGSM > FGSM \approx DI-FGSM > I-FGSM.

When VGG16 is the surrogate model and ResNet50 is the victim model for ImageNet, the sort of the attack success rates is VMI-FGSM (62.4%) > SI-NI-FGSM (56.6%) > MI-FGSM (46.5%) > DI-FGSM (38.1%) > FGSM (32.8%) > I-FGSM (27.8%), and the Figure 3-(3) shows that the sort of the cosine values is basically VMI-FGSM > FGSM > SI-NI-FGSM > MI-FGSM > DI-FGSM > I-FGSM.

When ResNet50 is the surrogate model and VGG16 is the victim model for CIFAR10, the sort of the attack success rates is VMI-FGSM (80.40%) > MI-FGSM (77.25%) > SI-NI-FGSM (73.00%) > DI-FGSM (67.65%) > I-FGSM (59.85%) > FGSM (44.20%), and the Figure 3-(4) shows that the sort of the cosine values is also basically VMI-FGSM > MI-FGSM > SI-NI-FGSM > DI-FGSM > I-FGSM > FGSM.

When ResNet50 is the surrogate model and VGG16 is the victim model for CIFAR100, the sort of the attack success rates is VMI-FGSM (84.40%) > MI-FGSM (77.35%) > SI-NI-FGSM (72.90%) > DI-FGSM (68.40%) > FGSM (64.80%) > I-FGSM (61.45%), and the Figure 3-(5) shows that the sort of the cosine values is also basically VMI-FGSM > MI-FGSM > SI-NI-FGSM > DI-FGSM > I-FGSM > FGSM.

When ResNet50 is the surrogate model and VGG16 is the victim model for ImageNet, the sort of the attack success rates is VMI-FGSM (69.1%) > SI-NI-FGSM (68.7%) > MI-FGSM (55.4%) > DI-FGSM (52.6%) > FGSM (42.6%) > I-FGSM (32.1%), and the Figure 3-(6) shows that the sort of the cosine values is also basically VMI-FGSM > FGSM > SI-NI-FGSM > MI-FGSM > DI-FGSM > I-FGSM.

In conclusion, by discussing the above six cases for CIFAR10/100 and ImageNet datasets, for the family of iterative fast gradient sign methods except for FGSM, Proposition 1 is correct with high

confidence. Therefore, decreasing the cosine value of the gradient angle between the surrogate model and the victim model can enhance the transferability of adversarial examples.

A.2 Proof of Proposition 2

Proposition 2: *When the victim model h is attacked by the white-box gradient-based attacks, the successful attacked adversarial examples prefer to be classified as the wrong categories with higher probability (i.e. the top- n wrong categories $\{y_{\tau_i} | i \leq \bar{n}\}$). Meanwhile, the higher the probability of the wrong category, the more likely the adversarial example is to be classified as this category.*

Proof 2 *To verify the correctness of Proposition 2, we explore the top- n wrong categories attack success rate (ASR) on I-FGSM at each iteration where the attack strength, number of iterations and step of size are $\epsilon, T, \alpha = 8/255, 10, 0.8/255$. Assuming that $ASR^{\bar{n}=n}$ denotes the top- n wrong categories ASR, and $\overline{ASR}^{\bar{n}=n}$ denotes the average top- n wrong categories, namely $\overline{ASR}^{\bar{n}=n} = \frac{ASR^{\bar{n}=n}}{\bar{n}}$. If the top- n wrong categories ASR is significantly higher than the average level (i.e. $\frac{1}{C-1}$ where C is the number of categories of the classification task.), namely $ASR^{\bar{n}=n} \gg \frac{1}{C-1}$, the previous sentence of Proposition 2 is correct with high confidence. If the average top- n_1 wrong categories ASR is higher than the average top- n_2 wrong categories ASR when $n_1 < n_2$, namely $\overline{ASR}^{\bar{n}=n_1} > \overline{ASR}^{\bar{n}=n_2}$ when $n_1 < n_2$, the last sentence of Proposition 2 is correct with high confidence.*

When VGG16 for CIFAR10 is attacked by I-FGSM, Figure 4-(1) shows that $ASR^{\bar{n}=5} > ASR^{\bar{n}=4} > ASR^{\bar{n}=3} > ASR^{\bar{n}=2} > ASR^{\bar{n}=1} \geq 69\% \gg \frac{1}{10-1}$ at each iteration. With the increase of the iteration t , $ASR^{\bar{n}=n}$ gradually increases and approaches 100%. Figure 5-(1) shows that $\overline{ASR}^{\bar{n}=1} > \overline{ASR}^{\bar{n}=2} > \overline{ASR}^{\bar{n}=3} > \overline{ASR}^{\bar{n}=4} > \overline{ASR}^{\bar{n}=5}$ at each iteration.

When ResNet50 for CIFAR10 is attacked by I-FGSM, Figure 4-(2) shows that $ASR^{\bar{n}=5} > ASR^{\bar{n}=4} > ASR^{\bar{n}=3} > ASR^{\bar{n}=2} > ASR^{\bar{n}=1} \geq 76\% \gg \frac{1}{10-1}$ at each iteration. With the increase of the iteration t , $ASR^{\bar{n}=n}$ gradually increases and approaches 100%. Figure 5-(2) shows that $\overline{ASR}^{\bar{n}=1} > \overline{ASR}^{\bar{n}=2} > \overline{ASR}^{\bar{n}=3} > \overline{ASR}^{\bar{n}=4} > \overline{ASR}^{\bar{n}=5}$ at each iteration.

When VGG16 for CIFAR100 is attacked by I-FGSM, Figure 4-(3) shows that $ASR^{\bar{n}=50} > ASR^{\bar{n}=20} > ASR^{\bar{n}=10} > ASR^{\bar{n}=5} > ASR^{\bar{n}=1} \geq 54\% \gg \frac{1}{100-1}$ at each iteration. With the increase of the iteration t , $ASR^{\bar{n}=n}$ gradually increases and approaches 100%. Figure 5-(1) shows that $\overline{ASR}^{\bar{n}=1} > \overline{ASR}^{\bar{n}=5} > \overline{ASR}^{\bar{n}=10} > \overline{ASR}^{\bar{n}=20} > \overline{ASR}^{\bar{n}=50}$ at each iteration.

When ResNet50 for CIFAR100 is attacked by I-FGSM, Figure 4-(4) shows that $ASR^{\bar{n}=50} > ASR^{\bar{n}=20} > ASR^{\bar{n}=10} > ASR^{\bar{n}=5} > ASR^{\bar{n}=1} \geq 52\% \gg \frac{1}{100-1}$ at each iteration. With the increase of the iteration t , $ASR^{\bar{n}=n}$ gradually increases and approaches 100%. Figure 5-(4) shows that $\overline{ASR}^{\bar{n}=1} > \overline{ASR}^{\bar{n}=5} > \overline{ASR}^{\bar{n}=10} > \overline{ASR}^{\bar{n}=20} > \overline{ASR}^{\bar{n}=50}$ at each iteration.

When VGG16 for ImageNet is attacked by I-FGSM, Figure 4-(5) shows that $ASR^{\bar{n}=50} > ASR^{\bar{n}=20} > ASR^{\bar{n}=10} > ASR^{\bar{n}=5} > ASR^{\bar{n}=1} \geq 33\% \gg \frac{1}{1000-1}$ at each iteration. With the increase of the iteration t , $ASR^{\bar{n}=n}$ gradually increases and approaches 100%. Figure 5-(5) shows that $\overline{ASR}^{\bar{n}=1} > \overline{ASR}^{\bar{n}=5} > \overline{ASR}^{\bar{n}=10} > \overline{ASR}^{\bar{n}=20} > \overline{ASR}^{\bar{n}=50}$ at each iteration.

When ResNet50 for ImageNet is attacked by I-FGSM, Figure 4-(6) shows that $ASR^{\bar{n}=50} > ASR^{\bar{n}=20} > ASR^{\bar{n}=10} > ASR^{\bar{n}=5} > ASR^{\bar{n}=1} \geq 43\% \gg \frac{1}{1000-1}$ at each iteration. With the increase of the iteration t , $ASR^{\bar{n}=n}$ gradually increases and approaches 100%. Figure 5-(6) shows that $\overline{ASR}^{\bar{n}=1} > \overline{ASR}^{\bar{n}=5} > \overline{ASR}^{\bar{n}=10} > \overline{ASR}^{\bar{n}=20} > \overline{ASR}^{\bar{n}=50}$ at each iteration.

In conclusion, by discussing the above six cases on CIFAR10/100 and ImageNet datasets, the Proposition 2 is correct with high confidence. Therefore, after knowing the output of the victim model, directly classifying the adversarial examples into the category in the top- n wrong categories can reduce the gradient perturbation of other wrong categories.

A.3 The detail design process of the WACE loss

According to Proposition 1, decreasing the gradient angle between the surrogate model f and the victim model h , i.e. the angle between $\nabla_x L_{CE}(x_t^{adv}, y_o; \theta_f)$ and $\nabla_x L_{CE}(x_t^{adv}, y_o; \theta_h)$, can enhance the transferability of adversarial examples.

According to the previous sentence of Proposition 2, because the successful attacked adversarial examples prefer to be classified as the wrong categories with higher probability, to avoid the gradient perturbation of other categories, besides maximizing the loss function $L_{CE}(x^{adv}, y_o; \theta_f)$, we also minimize the distance between the model output and the top- n wrong categories with higher probability, namely maximizing $L_{CE}(x^{adv}, y_o; \theta_f) - \sum_{i=1}^{\bar{n}} \frac{1}{\bar{n}} \cdot L_{CE}(x^{adv}, y_{\tau_i}; \theta_f)$ where each category in $\{y_{\tau_i} | i \leq \bar{n}\}$ is equally important.

According to the last sentence of Proposition 2, the higher the probability of the wrong category, the more likely the adversarial example is to be classified as this category. Therefore, we add weight to the distance calculation of the top- n wrong categories according to the logit of each category in the top- n wrong categories, namely maximizing $L_{CE}(x^{adv}, y_o; \theta_f) - \sum_{i=1}^{\bar{n}} \frac{e^{z_{\tau_i}}}{\sum_{j=1}^{\bar{n}} e^{z_{\tau_j}}} \cdot L_{CE}(x^{adv}, y_{\tau_i}; \theta_f)$.

Therefore, the WACE loss is:

$$L_{WACE}(x, y_o; \theta_f, \mathbf{Z}_h, \bar{n}) = L_{CE}(x, y_o; \theta_f) - \frac{1}{\bar{n}} \sum_{i=1}^{\bar{n}} \frac{e^{z_{\tau_i}}}{\sum_{j=1}^{\bar{n}} e^{z_{\tau_j}}} \cdot L_{CE}(x, y_{\tau_i}; \theta_f) \quad (11)$$

A.4 Proof of Theorem 1

Theorem 1: *The angle between $\nabla_x L_{WACE}(x_t^{adv}, y_o; \theta_f, \mathbf{Z}_h, \bar{n})$ and $\nabla_x L_{CE}(x_t^{adv}, y_o; \theta_h)$ is less than the angle between $\nabla_x L_{RCE}(x_t^{adv}, y_o; \theta_f)$ and $\nabla_x L_{CE}(x_t^{adv}, y_o; \theta_h)$, and the angle between $\nabla_x L_{CE}(x_t^{adv}, y_o; \theta_f)$ and $\nabla_x L_{CE}(x_t^{adv}, y_o; \theta_h)$.*

Proof 3 According to Proposition 2,

$$\begin{aligned} \nabla_x L_{CE}(x_t^{adv}, y_o; \theta_h) &= \frac{\partial L_{CE}}{\partial x_t^{adv}} = -\frac{\partial L_{CE}}{\partial z_o} \cdot \left(-\frac{\partial z_o}{\partial x_t^{adv}}\right) + \sum_{i=1(i \neq o)}^C \frac{\partial L_{CE}}{\partial z_i} \cdot \frac{\partial z_i}{\partial x_t^{adv}} \\ &= \frac{1}{\ln 2} \cdot \left(\left(1 - \frac{e^{z_o}}{\sum_{i=1}^C e^{z_i}}\right) \cdot \left(-\frac{\partial z_o}{\partial x_t^{adv}}\right) + \sum_{i=1(i \neq o)}^C \frac{e^{z_i}}{\sum_{j=1}^C e^{z_j}} \cdot \frac{\partial z_i}{\partial x_t^{adv}} \right) \\ &\approx \frac{1}{\ln 2} \cdot \left(\left(1 - \frac{e^{z_o}}{\sum_{i=1}^{\bar{n}} e^{z_i}}\right) \cdot \left(-\frac{\partial z_o}{\partial x_t^{adv}}\right) + \sum_{i=1}^{\bar{n}} \frac{e^{z_{\tau_i}}}{\sum_{j=1}^{\bar{n}} e^{z_{\tau_j}}} \cdot \frac{\partial z_{\tau_i}}{\partial x_t^{adv}} \right) \end{aligned} \quad (12)$$

Eq. 6, 7 and 9 in the main paper are the CE loss, the RCE loss and the WACE loss, respectively. The gradient of each loss w.r.t. x_t^{adv} on the surrogate model f is as follows, respectively.

$$\begin{aligned} \nabla_x L_{CE}(x_t^{adv}, y_o; \theta_f) &= \frac{\partial L_{CE}}{\partial x_t^{adv}} = -\frac{\partial L_{CE}}{\partial z_o} \cdot \left(-\frac{\partial z_o}{\partial x_t^{adv}}\right) + \sum_{i=1(i \neq o)}^C \frac{\partial L_{CE}}{\partial z_i} \cdot \frac{\partial z_i}{\partial x_t^{adv}} \\ &= \frac{1}{\ln 2} \cdot \left(\left(1 - \frac{e^{z_o}}{\sum_{i=1}^C e^{z_i}}\right) \cdot \left(-\frac{\partial z_o}{\partial x_t^{adv}}\right) + \sum_{i=1(i \neq o)}^C \frac{e^{z_i}}{\sum_{j=1}^C e^{z_j}} \cdot \frac{\partial z_i}{\partial x_t^{adv}} \right) \end{aligned} \quad (13)$$

$$\begin{aligned} \nabla_x L_{RCE}(x_t^{adv}, y_o; \theta_f) &= \frac{\partial L_{RCE}}{\partial x_t^{adv}} = -\frac{\partial L_{RCE}}{\partial z_o} \cdot \left(-\frac{\partial z_o}{\partial x_t^{adv}}\right) + \sum_{i=1(i \neq o)}^C \frac{\partial L_{RCE}}{\partial z_i} \cdot \frac{\partial z_i}{\partial x_t^{adv}} \\ &= \frac{1}{\ln 2} \cdot \left(\left(-\frac{\partial z_o}{\partial x_t^{adv}}\right) + \sum_{i=1}^C \frac{1}{C} \cdot \frac{\partial z_i}{\partial x_t^{adv}} \right) \end{aligned} \quad (14)$$

$$\begin{aligned}\nabla_x L_{WACE}(x_t^{adv}, y_o; \theta_f) &= \frac{\partial L_{WACE}}{\partial x_t^{adv}} = -\frac{\partial L_{WACE}}{\partial z_o} \cdot \left(-\frac{\partial z_o}{\partial x_t^{adv}}\right) + \sum_{i=1(i \neq o)}^C \frac{\partial L_{WACE}}{\partial z_i} \cdot \frac{\partial z_i}{\partial x_t^{adv}} \\ &= \frac{1}{\ln 2} \cdot \left(\left(-\frac{\partial z_o}{\partial x_t^{adv}}\right) + \sum_{i=1}^{\bar{n}} \frac{e^{z_{\tau_i}}}{\sum_{j=1}^{\bar{n}} e^{z_{\tau_j}}} \cdot \frac{\partial z_{\tau_i}}{\partial x_t^{adv}} \right)\end{aligned}\quad (15)$$

Assuming that x^{adv} is a successful attacked adversarial example and x_0^{adv} is correctly classified by the surrogate model f and the victim model h with almost 100% probability. **When the iteration t is equal to 0**, $(1 - \frac{e^{z_o}}{\sum_{i=1}^C e^{z_i}})$ is approximately 0 and $\frac{e^{z_i}}{\sum_{j=1}^C e^{z_j}}$ is approximately 0. Eq. 12 and 13 are transformed as follows, respectively.

$$\nabla_x L_{CE}(x_t^{adv}, y_o; \theta_h) \approx \frac{1}{\ln 2} \cdot \sum_{i=1}^{\bar{n}} \frac{e^{z_{\tau_i}}}{\sum_{j=1}^{\bar{n}} e^{z_{\tau_j}}} \cdot \frac{\partial z_{\tau_i}}{\partial x_t^{adv}} \quad (16)$$

$$\nabla_x L_{CE}(x_t^{adv}, y_o; \theta_f) \approx 0 \quad (17)$$

Therefore, according to Eq. 14, 15, 16 and 17, Theorem 1 is correct.

When the iteration t is greater than 0 and increases gradually, $(1 - \frac{e^{z_o}}{\sum_{i=1}^C e^{z_i}})$ is approximately 1 and $\sum_{i=1(i \neq o)}^C \frac{e^{z_i}}{\sum_{j=1}^C e^{z_j}}$ is approximately 1. Eq. 12 and 13 are transformed as follows, respectively.

$$\nabla_x L_{CE}(x_t^{adv}, y_o; \theta_h) \approx \frac{1}{\ln 2} \cdot \left(\left(-\frac{\partial z_o}{\partial x_t^{adv}}\right) + \sum_{i=1}^{\bar{n}} \frac{e^{z_{\tau_i}}}{\sum_{j=1}^{\bar{n}} e^{z_{\tau_j}}} \cdot \frac{\partial z_{\tau_i}}{\partial x_t^{adv}} \right) \quad (18)$$

$$\nabla_x L_{CE}(x_t^{adv}, y_o; \theta_f) \approx \frac{1}{\ln 2} \cdot \left(\left(-\frac{\partial z_o}{\partial x_t^{adv}}\right) + \sum_{i=1(i \neq o)}^C \frac{e^{z_i}}{\sum_{j=1}^C e^{z_j}} \cdot \frac{\partial z_i}{\partial x_t^{adv}} \right) \quad (19)$$

Therefore, according to Eq. 14, 15, 18 and 19, Theorem 1 is correct.

In conclusion, combining the above two cases, Theorem 1 is correct.

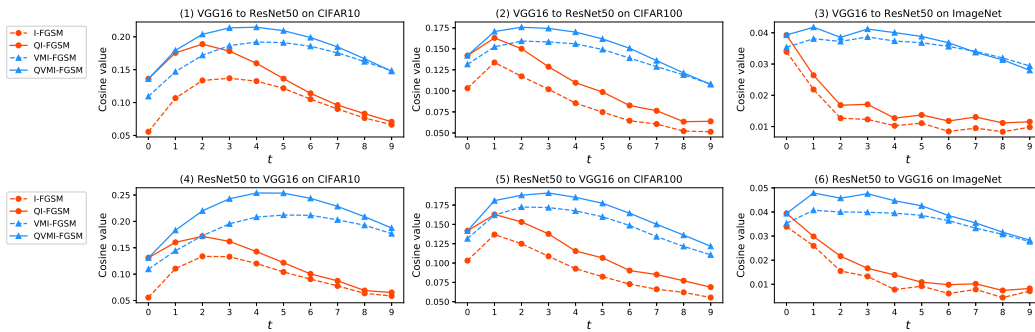


Figure 6: The cosine value of the gradient angle between the surrogate model and the victim model at each iteration t when the surrogate model is attacked by different methods for CIFAR10/100 and ImageNet. For example, in subfigure (1), VGG16 as the surrogate model and ResNet50 as the victim model are attacked by different transfer attacks for CIFAR10. The query prior-based attacks can significantly improve the cosine value of the gradient angle between the surrogate model and the victim model, i.e. decrease the gradient angle between the surrogate model and the victim model. Note that the attack strength $\epsilon = 8/255$.

Table 4: The attack success rates (%) on six naturally trained models for CIFAR10 using various transfer attacks and two query attacks with the attack strength $\epsilon = 8/255$. The adversarial examples are generated by ResNet50. * denotes the attack success rates under white-box attacks. **Average** means to calculate the average value except *. Note that $Q = 1$ in Q-FGSM.

Model	Attack	Loss	V16	V19	R50	WRN-16-4	D121	M-v2	Average
ResNet50	Square ($Q = 10$)	-	12.15	12.70	15.20	19.00	18.85	27.30	17.53
	PRGF ($Q = 10$)	-	4.25	4.15	26.95*	8.10	7.75	6.60	6.17
	FGSM	CE	44.20	46.20	65.50*	56.15	53.15	55.10	50.96
		RCE	37.95	38.95	54.70*	49.25	45.65	49.70	44.3
	Q-FGSM (Ours)	WACE	48.70	47.05	71.55*	59.75	56.20	58.00	53.94
		CE	59.85	62.55	99.85*	93.95	88.70	84.35	77.88
	I-FGSM	RCE	58.05	60.10	99.05*	90.60	86.15	82.25	75.43
		WACE	68.05	68.50	99.90*	96.90	92.80	89.45	83.14
	QI-FGSM (Ours)	CE	77.25	79.60	99.05*	93.60	89.70	87.15	85.46
		RCE	70.95	72.90	97.35*	88.50	84.90	82.55	79.96
	QMI-FGSM (Ours)	WACE	84.40	82.90	99.70*	97.00	93.55	91.85	89.94
		CE	67.65	69.65	98.20*	90.80	87.00	82.10	79.44
	DI-FGSM	RCE	63.75	63.65	94.50*	83.05	80.45	76.90	73.56
		WACE	75.05	73.20	99.25*	94.20	91.50	88.75	84.54
	QDI-FGSM (Ours)	CE	73.00	75.80	98.10*	92.35	89.95	86.45	83.51
		RCE	82.45	84.20	99.55*	96.75	94.85	92.35	90.12
	QSI-NI-FGSM (Ours)	WACE	87.55	87.85	99.85*	98.40	96.25	95.35	93.08
		CE	80.40	82.20	99.20*	94.60	90.80	88.95	87.39
	VMI-FGSM	RCE	77.75	78.05	97.50*	92.15	89.00	87.60	84.91
		WACE	88.60	86.10	99.65*	97.95	95.40	94.50	92.51

Table 5: The attack success rates (%) on six naturally trained models for CIFAR100 using various transfer attacks and two query attacks with the attack strength $\epsilon = 8/255$. The adversarial examples are generated by ResNet50. * denotes the attack success rates under white-box attacks. **Average** means to calculate the average value except *. Note that $Q = 1$ in Q-FGSM.

Model	Attack	Loss	V16	R50	RN50	WRN-16-4	D121	M-v2	Average
ResNet50	Square ($Q = 10$)	-	34.35	36.30	41.45	42.45	34.05	51.35	39.99
	PRGF ($Q = 10$)	-	8.70	43.65*	12.45	12.15	12.50	8.10	10.78
	FGSM	CE	64.80	83.40*	68.75	72.15	71.60	66.60	68.78
		RCE	63.85	81.75*	67.55	70.55	69.95	66.35	67.65
	Q-FGSM (Ours)	WACE	65.30	83.75*	69.65	72.80	72.60	67.65	69.6
		CE	61.45	99.00*	81.40	82.05	81.10	58.05	72.81
	I-FGSM	RCE	69.45	98.50*	84.10	85.80	84.35	68.00	78.34
		WACE	71.25	99.40*	88.55	90.30	87.65	70.50	81.65
	QI-FGSM (Ours)	CE	77.35	97.80*	85.55	86.70	85.70	74.05	81.87
		RCE	79.10	96.90*	86.50	88.10	87.10	78.20	83.8
	QMI-FGSM (Ours)	WACE	80.90	98.80*	89.45	91.40	90.05	79.35	86.23
		CE	68.40	97.55*	83.40	83.05	81.25	65.85	76.39
	DI-FGSM	RCE	72.55	96.05*	83.50	85.25	83.10	71.70	79.22
		WACE	74.70	98.25*	88.25	89.65	88.30	75.15	83.21
	QDI-FGSM (Ours)	CE	72.90	97.00*	82.60	84.85	82.65	70.75	78.75
		RCE	84.85	99.55*	91.70	92.75	92.00	84.05	89.07
	QSI-NI-FGSM (Ours)	WACE	86.10	99.65*	93.70	93.75	93.90	82.20	89.93
		CE	84.40	98.20*	88.75	90.35	89.25	80.70	86.69
	VMI-FGSM	RCE	84.00	97.90*	90.45	91.20	90.55	82.70	87.78
		WACE	87.05	98.95*	92.70	94.35	93.20	84.60	90.38

A.5 The reduction of the gradient angle with the WACE loss

To verify that the WACE loss can reduce the gradient angle between the surrogate model and the victim model, we compare the cosine value of the gradient angle between the family of iterative FGSM and their query prior-based version. As shown in Figure 6, for CIFAR10/100 and ImageNet, at each iteration, the cosine value of the gradient angle between the surrogate model and the victim model on the family of iterative FGSM are smaller than that on their query prior-based version. Therefore, the WACE loss can reduce the gradient angle between the surrogate model and the victim model.

B Additional experiments

We add the experimental results by using the other surrogate models or increasing the attack strength (i.e. $\epsilon = 16/255$) on CIFAR10/100 and ImageNet.

Table 6: The attack success rates (%) on six naturally trained models and two adversarially trained models for ImageNet using various transfer attacks and two query attacks with the attack strength $\epsilon = 8/255$. The adversarial examples are generated by VGG16. * denotes the attack success rates under white-box attacks. **Avg.** means to calculate the average value of the naturally trained models except *. Note that $Q = 1$ in Q-FGSM.

Model	Attack	Loss	V16	V19	R50	R152	I-v3	M-v2	Avg.	a-I-v3	ae-IR-v2
VGG16	Square ($Q = 0$)	-	40.2	34.5	16.5	12.4	17.9	34.1	25.9	12.3	11.2
	Square ($Q = 1$)	-	41.2	35.7	17.8	13.5	19.2	35.1	27.1	14.5	12.4
	Square ($Q = 10$)	-	47.7	41.6	23.2	16.2	23.6	41.3	32.3	20.3	16.8
	PRGF ($Q = 10$)	-	88.2*	21.1	4.3	-	2.7	6.1	8.6	2.5	1.0
	FGSM	CE	95.6*	72.8	32.8	24.6	26.0	42.0	39.6	18.0	10.1
		RCE	95.0*	67.0	27.6	18.2	21.1	38.3	34.4	17.0	7.9
	Q-FGSM (Ours)	WACE	96.4*	72.7	33.9	24.4	26.4	43.9	40.3	18.1	10.4
	I-FGSM	CE	99.4*	87.9	27.8	18.4	15.0	37.3	37.3	7.8	3.9
		RCE	100*	82.2	18.4	12.2	10.4	28.7	30.4	7.0	3.6
	QI-FGSM (Ours)	WACE	100*	90.6	33.9	22.6	21.2	46.6	43.0	8.5	5.9
	MI-FGSM	CE	99.4*	95.8	46.5	33.5	32.7	58.3	53.4	13.8	7.2
		RCE	100*	94.5	38.3	27.3	28.3	55.4	48.8	14.0	7.2
	QMI-FGSM (Ours)	WACE	100*	96.5	52.4	39.5	36.7	65.0	58.0	16.1	9.2
	DI-FGSM	CE	99.6*	94.1	38.1	26.2	27.0	52.3	47.5	8.8	5.4
		RCE	99.9*	90.9	27.6	17.7	20.2	44.8	40.2	9.0	4.5
	QDI-FGSM (Ours)	WACE	100*	94.9	45.6	33.5	34.0	61.0	53.8	10.7	7.8
	SI-NI-FGSM	CE	100*	98.0	56.6	41.8	43.8	70.3	62.1	17.7	11.5
		RCE	100*	97.7	54.3	41.1	40.5	70.4	60.8	16.9	10.3
	QSI-NI-FGSM (Ours)	WACE	100*	97.5	64.5	51.6	47.3	75.4	67.3	21.1	13.9
	VMI-FGSM	CE	99.4*	98.0	62.4	48.5	43.6	72.8	65.1	17.5	11.3
		RCE	100*	96.1	55.4	42.3	41.3	68.4	60.7	16.7	10.4
	QVMI-FGSM (Ours)	WACE	100*	98.1	69.2	54.6	50.5	78.2	70.1	19.8	14.5

Table 7: The attack success rates (%) on six naturally trained models for CIFAR10 using various transfer attacks and two query attacks with the attack strength $\epsilon = 16/255$. The adversarial examples are generated by VGG16. * denotes the attack success rates under white-box attacks. **Average** means to calculate the average value except *. Note that $Q = 1$ in Q-FGSM.

Model	Attack	Loss	V16	V19	R50	WRN-16-4	D121	M-v2	Average
VGG16	Square ($Q = 10$)	-	44.80	42.55	43.50	57.75	58.10	65.05	51.96
	PRGF ($Q = 10$)	-	39.30*	12.80	10.55	13.60	11.70	12.60	12.25
	FGSM	CE	70.50*	64.65	65.70	67.60	61.75	76.25	67.19
		RCE	66.35*	62.05	63.00	64.75	59.40	74.20	64.68
	Q-FGSM (Ours)	WACE	77.70*	67.50	69.75	71.45	67.25	79.35	71.06
	I-FGSM	CE	99.75*	87.60	79.10	89.25	84.05	84.90	84.98
		RCE	99.45*	87.15	80.75	89.40	85.25	86.70	85.85
	QI-FGSM (Ours)	WACE	99.90*	91.60	85.95	94.30	90.75	90.75	90.67
	MI-FGSM	CE	98.90*	94.00	90.00	93.45	91.15	90.75	91.87
		RCE	98.50*	93.15	90.00	93.15	91.40	91.45	91.83
	QMI-FGSM (Ours)	WACE	99.35*	95.55	93.10	96.65	94.50	94.90	94.94
	DI-FGSM	CE	98.10*	91.90	85.95	91.85	88.70	89.95	89.67
		RCE	97.35*	90.35	84.65	90.25	87.70	89.45	88.48
	QDI-FGSM (Ours)	WACE	99.00*	94.25	91.50	96.00	94.35	95.60	94.34
	SI-NI-FGSM	CE	99.90*	96.25	94.25	96.70	94.20	94.05	95.09
		RCE	99.70*	97.70	96.20	98.05	96.40	97.50	97.17
	QSI-NI-FGSM (Ours)	WACE	99.95*	99.30	97.70	98.80	98.40	98.10	98.46
	VMI-FGSM	CE	99.85*	97.35	95.10	96.80	95.40	96.15	96.16
		RCE	99.50*	97.30	96.25	97.40	96.85	97.25	97.01
	QVMI-FGSM (Ours)	WACE	99.80*	98.70	97.80	99.25	98.35	99.00	98.62

B.1 Comparison with or without the query priors

This section is an extension of Section 4.2 in the main paper.

B.1.1 Attacking a naturally trained model

We set the surrogate model as ResNet50 for CIFAR10/100 and VGG16 for ImageNet with the attack strength $\epsilon = 8/255$ to attack six naturally trained models. As shown in Tables 4, 5 and 6, the average increase of the ASR is 2.98% on Q-FGSM and 4.48 to 9.57% on the other five transfer attacks for CIFAR10, 0.82% on Q-FGSM and 3.69 to 11.18% on the other five transfer attacks for CIFAR100, 0.7% on Q-FGSM and 4.6 to 6.3% on the other five transfer attacks for ImageNet.

Table 8: The attack success rates (%) on six naturally trained models for CIFAR100 using various transfer attacks and two query attacks with the attack strength $\epsilon = 16/255$. The adversarial examples are generated by VGG16. * denotes the attack success rates under white-box attacks. **Average** means to calculate the average value except *. Note that $Q = 1$ in Q-FGSM.

Model	Attack	Loss	V16	R50	RN50	WRN-16-4	D121	M-v2	Average	
VGG16	Square ($Q = 10$)	-	76.10	72.20	74.25	78.70	71.10	83.85	76.03	
	PRGF ($Q = 10$)	-	63.65*	15.45	18.35	17.60	14.30	14.85	16.11	
	FGSM	CE	91.50*	84.80	85.90	87.25	84.80	86.75	85.9	
		RCE	90.95*	83.95	85.40	86.50	84.00	86.35	85.24	
	Q-FGSM (Ours)	WACE	91.60*	85.70	86.55	88.10	85.15	87.50	86.6	
		CE	100*	68.25	74.50	78.40	71.35	69.60	72.42	
	I-FGSM	RCE	100*	66.75	73.50	78.60	72.20	74.25	73.06	
		WACE	100*	77.85	83.40	86.30	81.30	79.40	81.65	
	QI-FGSM (Ours)	CE	100*	87.95	88.50	91.10	87.35	86.15	88.21	
		RCE	100*	88.85	90.15	92.85	89.50	89.50	90.17	
	MI-FGSM	WACE	100*	92.65	92.20	95.35	92.00	90.85	92.61	
		CE	99.75*	77.55	81.25	86.25	80.10	79.50	80.93	
	DI-FGSM	RCE	99.70*	78.40	82.75	86.30	81.10	83.00	82.31	
		WACE	99.95*	85.80	88.60	92.10	87.30	87.30	88.22	
	QDI-FGSM (Ours)	CE	99.85*	88.90	90.40	92.45	89.40	89.60	90.15	
		RCE	100*	91.10	92.55	93.30	92.10	93.40	92.49	
	QSI-NI-FGSM (Ours)	WACE	100*	93.10	92.85	95.95	93.30	92.75	93.59	
		CE	100*	93.25	92.30	95.10	92.75	91.65	93.01	
	VMI-FGSM	RCE	100*	93.95	93.80	95.75	93.75	93.65	94.18	
		WACE	99.95*	95.75	96.05	96.50	94.45	93.85	95.32	

Table 9: The attack success rates (%) on six naturally trained models and two adversarially trained models for ImageNet using various transfer attacks and two query attacks with the attack strength $\epsilon = 16/255$. The adversarial examples are generated by VGG16. * denotes the attack success rates under white-box attacks. **Avg.** means to calculate the average value of the naturally trained models except *. Note that $Q = 1$ in Q-FGSM.

Model	Attack	Loss	V16	V19	R50	R152	I-v3	M-v2	Avg.	a-I-v3	ae-IR-v2	
VGG16	Square ($Q = 0$)	-	79.0	72.6	39.6	27.6	38.4	70.9	54.7	32.2	27.6	
	Square ($Q = 1$)	-	79.4	73.3	41.1	29.8	39.7	71.7	55.8	34.8	29.1	
	Square ($Q = 10$)	-	84.0	80.2	51.5	40.1	50.7	79.4	64.3	46.4	38.2	
	PRGF ($Q = 10$)	-	94.5*	38.9	10.3	-	5.7	13.1	17.0	5.8	2.1	
	FGSM	CE	94.8*	82.9	47.4	36.4	35.8	61.6	52.8	32.0	16.8	
		RCE	95.4*	81.5	43.4	32.1	34.1	61.5	50.5	31.5	14.7	
	Q-FGSM (Ours)	WACE	95.8*	82.4	47.9	35.9	34.8	62.8	52.8	32.7	15.9	
		CE	99.4*	97.2	46.2	31.7	28.1	58.8	52.4	13.9	7.5	
	I-FGSM	RCE	100*	96.3	35.9	25.4	22.2	52.2	46.4	14.0	6.5	
		WACE	100*	97.6	53.4	39.2	32.4	66.4	57.8	15.4	8.2	
	MI-FGSM	CE	99.4*	98.7	69.0	54.2	51.1	79.8	70.6	24.5	14.6	
		RCE	100*	99.2	66.7	50.9	48.2	81.1	69.2	24.2	13.0	
	QMI-FGSM (Ours)	WACE	100*	99.1	73.0	60.7	54.9	81.7	73.9	25.5	16.1	
		CE	99.6*	98.6	60.2	44.8	44.6	73.8	64.4	15.6	9.2	
	DI-FGSM	RCE	100*	97.9	50.2	38.1	37.5	68.3	58.4	14.4	8.3	
		WACE	100*	98.7	67.1	53.3	50.1	80.9	70.0	17.6	12.3	
	QDI-FGSM (Ours)	CE	100*	99.7	86.0	73.1	70.8	91.7	84.3	32.5	20.9	
		RCE	100*	99.6	85.1	71.0	67.6	91.1	82.9	28.4	18.5	
	QSI-NI-FGSM (Ours)	WACE	100*	99.5	84.7	72.3	68.4	90.2	83.0	33.5	22.5	
		CE	99.8*	99.4	83.4	72.2	65.8	88.3	81.8	32.5	22.2	
	VMI-FGSM	RCE	100*	99.4	84.9	70.9	67.2	89.5	82.4	32.7	22.9	
		WACE	100*	99.7	87.2	78.4	70.3	90.6	85.2	37.3	28.0	

We set the surrogate model as VGG16 for CIFAR10/100 and ImageNet with the attack strength $\epsilon = 16/255$ to attack six naturally trained models. As shown in Tables 7, 8 and 9, the average increase of the ASR is 3.87% on Q-FGSM and 2.46 to 5.69% on the other five transfer attacks for CIFAR10, 0.7% on Q-FGSM and 2.31 to 9.23% on the other five transfer attacks for CIFAR100, 3.3 to 5.6% on the other four transfer attacks (i.e., QI-FGSM, QMI-FGSM, QDI-FGSM, QVMI-FGSM) for ImageNet. The average attack success rate is the same on Q-FGSM and decreases by 1.3% on QSI-NI-FGSM for ImageNet.

We set the surrogate model as ResNet50 for CIFAR10/100 and ImageNet with the attack strength $\epsilon = 16/255$ to attack six naturally trained models. As shown in Tables 10, 11 and 12, the average increase of the ASR is 1.79% on Q-FGSM and 0.93 to 2.33% on the other five transfer attacks for CIFAR10, 0.51% on Q-FGSM and 1.61 to 6.04% on the other five transfer attacks for CIFAR100,

Table 10: The attack success rates (%) on six naturally trained models for CIFAR10 using various transfer attacks and two-query attacks with the attack strength $\epsilon = 16/255$. The adversarial examples are generated by ResNet50. * denotes the attack success rates under white-box attacks. **Average** means to calculate the average value except *. Note that $Q = 1$ in Q-FGSM.

Model	Attack	Loss	V16	V19	R50	WRN-16-4	D121	M-v2	Average
ResNet50	Square ($Q = 10$)	-	42.10	43.50	45.00	57.70	57.30	66.20	51.97
	PRGF ($Q = 10$)	-	9.25	10.40	43.45*	19.25	16.55	15.40	14.17
	FGSM	CE	66.60	69.55	80.25*	75.85	73.95	77.95	72.78
		RCE	60.90	64.35	74.90*	71.35	68.30	76.00	68.18
	Q-FGSM (Ours)	WACE	71.25	71.00	82.70*	77.35	74.05	79.30	74.59
		CE	84.55	86.70	100*	99.05	97.55	94.50	92.47
	I-FGSM	RCE	84.50	85.60	100*	99.15	96.70	95.50	92.29
		WACE	89.30	90.15	100*	99.70	98.60	96.25	94.8
	QI-FGSM (Ours)	CE	95.50	96.45	99.95*	99.50	98.75	97.20	97.48
		RCE	94.30	95.35	99.85*	98.90	97.90	96.25	96.54
	QMI-FGSM (Ours)	WACE	97.35	97.45	100*	99.80	99.20	98.25	98.41
		CE	93.10	94.20	99.95*	99.05	97.80	96.45	96.12
	DI-FGSM	RCE	91.35	91.65	99.45*	98.15	97.05	96.40	94.92
		WACE	95.95	95.00	100*	99.80	99.20	98.45	97.68
	QDI-FGSM (Ours)	CE	96.50	97.10	99.95*	99.55	98.75	97.85	97.95
		RCE	98.25	98.75	100*	99.95	99.70	99.35	99.2
	QSI-NI-FGSM (Ours)	WACE	98.70	98.70	100*	100	99.90	98.80	99.22
		CE	96.80	97.10	99.95*	99.25	98.85	97.40	97.88
	VMI-FGSM	RCE	97.65	97.70	99.80*	99.30	99.20	98.90	98.55
		WACE	98.55	98.60	100*	99.75	99.70	99.30	99.18

Table 11: The attack success rates (%) on six naturally trained models for CIFAR100 using various transfer attacks and two query attacks with the attack strength $\epsilon = 16/255$. The adversarial examples are generated by ResNet50. * denotes the attack success rates under white-box attacks. **Average** means to calculate the average value except *. Note that $Q = 1$ in Q-FGSM.

Model	Attack	Loss	V16	R50	RN50	WRN-16-4	D121	M-v2	Average
ResNet50	Square ($Q = 10$)	-	73.25	74.15	74.90	77.95	71.80	84.80	76.14
	PRGF ($Q = 10$)	-	18.05	60.95*	26.65	26.40	25.00	17.15	22.65
	FGSM	CE	84.75	91.15*	86.05	88.25	85.80	86.60	86.29
		RCE	83.55	90.90*	85.80	87.65	85.25	86.55	85.76
	Q-FGSM (Ours)	WACE	84.30	91.90*	87.00	89.30	86.00	87.40	86.8
		CE	80.55	99.90*	91.65	93.45	90.85	75.80	86.46
	I-FGSM	RCE	86.80	99.90*	94.30	95.85	94.50	85.95	91.48
		WACE	88.20	99.90*	96.05	96.95	95.60	85.70	92.5
	QI-FGSM (Ours)	CE	92.10	99.70*	93.95	96.25	94.75	89.00	93.21
		RCE	94.80	99.45*	96.00	97.10	96.00	93.20	95.42
	QMI-FGSM (Ours)	WACE	94.70	99.80*	97.05	98.55	97.00	91.90	95.84
		CE	87.65	99.60*	93.75	95.00	93.90	83.45	90.75
	DI-FGSM	RCE	91.70	99.30*	94.50	96.10	94.60	89.10	93.2
		WACE	92.85	99.80*	97.00	97.80	97.05	90.95	95.13
	QDI-FGSM (Ours)	CE	91.95	99.70*	93.70	96.40	95.50	91.40	93.79
		RCE	97.50	100*	98.35	98.80	98.95	97.35	98.19
	QSI-NI-FGSM (Ours)	WACE	96.90	100*	98.65	98.65	98.85	95.25	97.66
		CE	95.85	99.75*	96.20	98.15	97.20	94.15	96.31
	VMI-FGSM	RCE	97.25	99.70*	97.90	98.30	97.80	95.50	97.35
		WACE	97.40	99.85*	98.05	99.25	98.60	96.30	97.92

0.5% on Q-FGSM and 4.2 to 10% on the other four transfer attacks (i.e., QI-FGSM, QMI-FGSM, QDI-FGSM and QVMI-FGSM) for ImageNet. The average attack success rate decreases by 0.8% on QSI-NI-FGSM for ImageNet.

In Conclusion, through the comparison with or without the query priors, at the low attack strength, i.e. $\epsilon = 8/255$, the query prior-based attacks can significantly enhance the transferability of adversarial examples to attack the naturally trained models. At the high attack strength, i.e. $\epsilon = 16/255$, the most of query prior-based attacks can enhance the transferability of adversarial examples, but the average ASR of QSI-NI-FGSM has a slight decrease on ImageNet.

B.1.2 Attacking an adversarially trained model

We set the surrogate model as VGG16 for ImageNet with the attack strength $\epsilon = 8/255$ to attack two adversarially trained models. As shown in Table 6, the increase of the ASR is 0.1 to 0.3% on Q-FGSM and 0.7 to 3.4% on the other five transfer attacks.

Table 12: The attack success rates (%) on six naturally trained models and two adversarially trained models for ImageNet using various transfer attacks and two query attacks with the attack strength $\epsilon = 16/255$. The adversarial examples are generated by ResNet50. * denotes the attack success rates under white-box attacks. **Avg.** means to calculate the average value of the naturally trained models except *. Note that $Q = 1$ in Q-FGSM.

Model	Attack	Loss	V16	V19	R50	R152	I-v3	M-v2	Avg.	a-I-v3	ae-IR-v2
ResNet50	Square ($Q = 0$)	-	77.8	73.2	42.2	30.7	40.4	72.2	56.1	35.1	30.4
	Square ($Q = 1$)	-	78.5	74.6	44.0	33.5	41.9	73.0	57.6	37.3	32.2
	Square ($Q = 10$)	-	83.8	80.6	55.8	43.4	51.9	79.5	65.8	47.3	40.1
	PRGF ($Q = 10$)	-	12.1	11.0	88.9*	-	6.7	13.6	10.9	5.9	3.6
	FGSM	CE	66.7	63.0	87.1*	52.8	41.4	61.4	57.1	32.7	19.0
		RCE	62.8	61.3	80.6*	44.4	38.1	60.7	53.5	31.8	18.6
	Q-FGSM (Ours)	WACE	66.9	63.8	86.8*	51.8	42.3	63.3	57.6	33.7	21.3
	I-FGSM	CE	49.3	46.8	100*	66.5	29.2	53.6	49.1	15.1	10.0
		RCE	52.4	49.0	100*	60.9	30.2	52.4	49.0	15.9	9.6
	QI-FGSM (Ours)	WACE	61.8	57.1	100*	75.6	36.4	64.6	59.1	17.4	11.2
	MI-FGSM	CE	77.1	75.7	100*	84.8	56.2	75.5	73.9	27.8	18.7
		RCE	82.8	81.3	100*	84.0	57.9	80.1	77.2	28.5	19.2
	QMI-FGSM (Ours)	WACE	81.3	78.9	100*	88.6	61.0	82.5	78.5	28.6	23.5
	DI-FGSM	CE	73.1	71.0	100*	83.7	56.7	75.7	72.0	19.3	13.5
		RCE	75.8	72.3	100*	81.3	54.6	74.8	71.8	18.7	13.8
	QDI-FGSM (Ours)	WACE	81.0	78.5	100*	89.8	62.7	83.3	79.1	24.2	17.0
	SI-NI-FGSM	CE	91.8	91.2	100*	96.6	79.3	91.9	90.2	41.2	30.0
		RCE	93.1	94.3	100*	97.5	79.5	94.4	91.8	37.0	26.7
	QSI-NI-FGSM (Ours)	WACE	90.5	89.2	100*	96.3	78.0	92.8	89.4	38.8	31.4
	VMI-FGSM	CE	89.3	88.3	100*	95.7	74.2	88.6	87.2	38.1	32.6
RCE		91.7	91.2	100*	96.5	80.1	91.2	90.1	44.2	38.9	
QVMI-FGSM (Ours)	WACE	91.5	91.8	100*	97.6	82.3	93.7	91.4	47.0	40.5	

Table 13: The attack success rates (%) on adversarial Inception-v3 for ImageNet using various transfer attacks and a query attack with the attack strength $\epsilon = 8/255$. The adversarial examples are generated by adversarial ensemble Inception-Resnet-v2. Note that $Q = 1$ in Q-FGSM and $Q = 5$ in the other attacks.

		a-I-v3					
Attack	Square	Q-FGSM	QI-FGSM	QMI-FGSM	QDI-FGSM	QSI-NI-FGSM	QVMI-FGSM
ae-IR-v2	16.9	23.2	13.4	22.9	17.7	24.5	28.7

We set the surrogate model as VGG16 for ImageNet with the attack strength $\epsilon = 16/255$ to attack two adversarially trained models, As shown in Table 9, the ASR increases by 0.7% on Q-FGSM for adversarial Inception-v3, but the ASR decreases by 0.9% on Q-FGSM for adversarial ensemble Inception-Resnet-v2. The increase of the ASR is 0.7 to 5.8% on the other five transfer attacks for the two adversarially trained models.

We set the surrogate model as ResNet50 for ImageNet with the attack strength $\epsilon = 16/255$ to attack two adversarially trained models, As shown in Table 12, the increase of the ASR is 1 to 2.3% on Q-FGSM and 0.8 to 8.9% on the other five transfer attacks. However, for adversarial Inception-v3, the ASR decreases by 2.4% on QSI-NI-FGSM.

In Conclusion, through the comparison with or without the query priors, at the low attack strength, i.e. $\epsilon = 8/255$, the query prior-based attacks except for Q-FGSM can enhance the transferability of adversarial examples to attack the adversarially trained models. At the high attack strength, i.e. $\epsilon = 16/255$, the query prior-based attacks except for Q-FGSM can enhance the transferability of adversarial examples to attack the adversarially trained models, but the existence of QSI-NI-FGSM reduces the attack success rate.

B.2 Comparison between different loss functions

This section is an extension of Section 4.3 in the main paper.

B.2.1 Attacking a naturally trained model

We set the surrogate model as ResNet50 for CIFAR10/100 and VGG16 for ImageNet with the attack strength $\epsilon = 8/255$ to attack six naturally trained models. As shown in Tables 4, 5 and 6, the average

Table 14: The attack success rates (%) on adversarial Inception-v3 for ImageNet using various transfer attacks and a query attack with the attack strength $\epsilon = 16/255$. The adversarial examples are generated by adversarial ensemble Inception-Resnet-v2. Note that $Q = 1$ in Q-FGSM and $Q = 5$ in the other attacks.

a-I-v3							
Attack	Square	Q-FGSM	QI-FGSM	QMI-FGSM	QDI-FGSM	QSI-NI-FGSM	QVMI-FGSM
ae-IR-v2	39.4	41.3	21.4	36.3	28.3	38.5	46.9

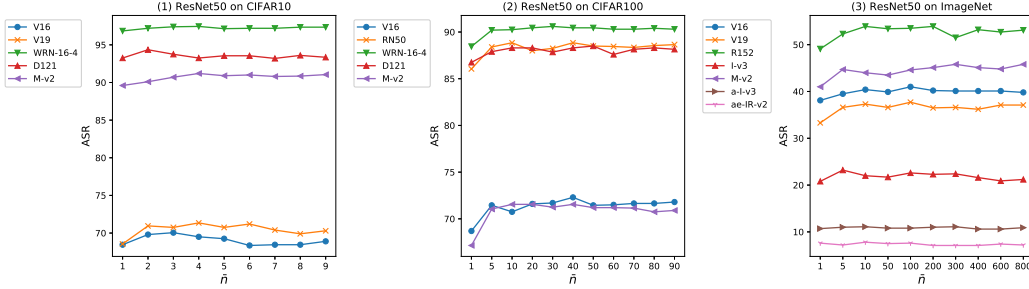


Figure 7: The attack success rates (%) on the victim models with adversarial examples generated by QI-FGSM ($\epsilon = 8/255$) for CIFAR10/100 and ImageNet (the surrogate model is ResNet50) when varying the number of the top- \bar{n} wrong categories \bar{n} .

increase of the ASR is 9.64% on Q-FGSM and 2.96 to 10.98 on the other five transfer attacks for CIFAR10, 1.95% on Q-FGSM and 0.86 to 3.99% on the other five transfer attacks for CIFAR100, 5.9% on Q-FGSM and 6.5 to 13.6% on the other five transfer attacks for ImageNet.

We set the surrogate model as VGG16 for CIFAR10/100 and ImageNet with the attack strength $\epsilon = 16/255$ to attack six naturally trained models. As shown in Tables 7, 8 and 9, the average increase of the ASR is 6.38% on Q-FGSM and 1.29 to 5.86% on the other five transfer attacks for CIFAR10, 1.36% on Q-FGSM and 1.1 to 8.59% on the other five transfer attacks for CIFAR100, 1.7% on Q-FGSM, 0.1 to 11.6% on the other five transfer attacks for ImageNet.

We set the surrogate model as ResNet50 for CIFAR10/100 and ImageNet with the attack strength $\epsilon = 16/255$ to attack six naturally trained models. As shown in Tables 10, 11 and 12, the average increase of the ASR is 6.41% on Q-FGSM and 0.02 to 2.76% on the other five transfer attacks for CIFAR10, 1.04% on Q-FGSM and 0.42 to 1.93% on the other four transfer attacks (i.e., QI-FGSM, QMI-FGSM, QDI-FGSM, QVMI-FGSM) for CIFAR100, 4.1% on Q-FGSM and 1.3 to 10.1% on the other four transfer attacks (i.e., QI-FGSM, QMI-FGSM, QDI-FGSM, QVMI-FGSM) for ImageNet. The average ASR decreases by 0.53% and 2.4% on QSI-NI-FGSM for CIFAR100 and ImageNet, respectively.

In Conclusion, through the comparison between different loss functions (i.e. the RCE loss), at the low attack strength, i.e. $\epsilon = 8/255$, the query prior-based attacks can significantly enhance the transferability of adversarial examples to attack the naturally trained models. At the high attack strength, i.e. $\epsilon = 16/255$, the most of query prior-based attacks can enhance the transferability of adversarial examples, but the average ASR of QSI-NI-FGSM has a slight decrease for CIFAR100 and ImageNet when the surrogate model is ResNet50.

B.2.2 Attacking an adversarially trained model

We set the surrogate model as VGG16 for ImageNet with the attack strength $\epsilon = 8/255$ to attack two adversarially trained models. As shown in Table 6, the increase of the ASR is 1.1 to 2.5% on Q-FGSM and 1.5 to 4.2% on the other five transfer attacks.

We set the surrogate model as VGG16 for ImageNet with the attack strength $\epsilon = 16/255$ to attack two adversarially trained models. As shown in Table 9, the increase of the ASR is 1.2% on Q-FGSM and 1.3 to 5.1% on the other five transfer attacks.

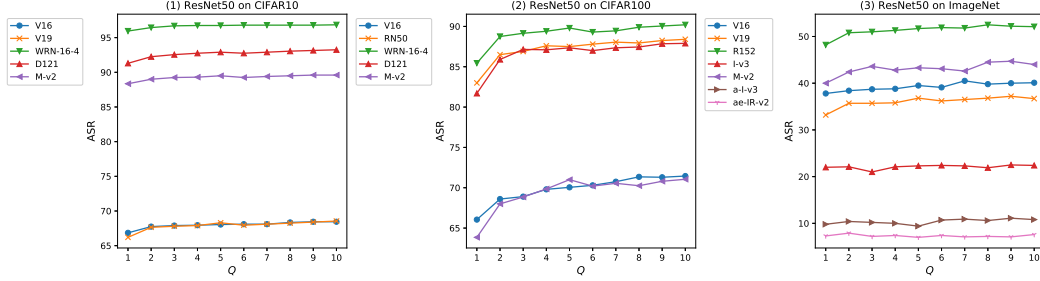


Figure 8: The attack success rates (%) on the victim models with adversarial examples generated by QI-FGSM ($\epsilon = 8/255$) for CIFAR10/100 and ImageNet (the surrogate model is ResNet50) when varying the number of queries Q .

We set the surrogate model as ResNet50 for ImageNet with the attack strength $\epsilon = 16/255$ to attack two adversarially trained models, As shown in Table 12, the increase of the ASR is 1.9 to 2.7% on Q-FGSM and 0.1 to 5.5% on the other five transfer attacks.

In Conclusion, through the comparison between different loss functions, whether the attack strength is low or high, the query prior-based attacks can enhance the transferability of adversarial examples to attack the adversarially trained models.

B.3 Comparison with current query attacks

This section is an extension of Section 4.4 in the main paper.

B.3.1 Black-box query attacks

We set the surrogate model as ResNet50 for CIFAR10/100 and VGG16 for ImageNet with the attack strength $\epsilon = 8/255$ to attack six naturally trained models. As shown in Tables 4, 5 and 6, by comparing the best query prior-based attacks with Square, the average increase of the ASR is 75.55% for CIFAR10, 50.39% for CIFAR100 and 37.8% for ImageNet. When attacking two adversarially trained models for ImageNet, by comparing the best query prior-based attacks with Square, the increase of the ASR is 0.8% for attacking adversarial Inception-v3, but the ASR decreases by 2.3% for attacking adversarial ensemble Inception-Resnet-v2. In fact, when the query number of Square is 0 (i.e. $Q = 0$), the ASR of Square is basically equal to that of the transfer attacks (i.e. the family of FGSMs) for attacking adversarial ensemble Inception-Resnet-v2.

We set the surrogate model as VGG16 for CIFAR10/100 and ImageNet with the attack strength $\epsilon = 16/255$ to attack six naturally trained models. As shown in Tables 7, 8 and 9, by comparing the best query prior-based attacks with Square, the average increase of the ASR is 46.66% for CIFAR10, 19.29% for CIFAR100 and 20.9% for ImageNet. When attacking two adversarially trained models for ImageNet, by comparing the best query prior-based attacks with Square, the ASR of the query prior-based attacks is smaller than that of Square. When the query number of Square is 0 (i.e. $Q = 0$), the ASR of Square is greater or equal to that of the transfer attacks (i.e. the family of FGSMs) for both adversarial Inception-v3 and adversarial ensemble Inception-Resnet-v2.

We set the surrogate model as ResNet50 for CIFAR10/100 and ImageNet with the attack strength $\epsilon = 16/255$ to attack six naturally trained models. As shown in Tables 10, 11 and 12, by comparing the best query prior-based attacks with Square, the average increase of the ASR is 47.25% for CIFAR10, 24.78% for CIFAR100 and 25.6% for ImageNet. When attacking two adversarially trained models for ImageNet, by comparing the best query prior-based attacks with Square, the ASR of the query prior-based attacks is basically equal to that of Square. When the query number of Square is 0 (i.e. $Q = 0$), the ASR of Square is greater or basically equal to that of the transfer attacks (i.e. the family of FGSMs) for both adversarial Inception-v3 and adversarial ensemble Inception-Resnet-v2.

To highlight the advantages of the query prior-based attacks for attacking the adversarially trained models, we set adversarial ensemble Inception-Resnet-v2 as the surrogate model rather than the

naturally trained models (i.e. VGG16 or ResNet50) and adversarial Inception-v3 as the victim model, and reduce the query number from 10 to 5 (i.e. $Q = 5$). As shown in Tables 13 and 14, when the attack strength is $8/255$, by comparing the best query prior-based attacks with Square, the increase of the ASR is 11.8%. When the attack strength is $16/255$, the increase of the ASR is 7.5%.

In conclusion, through the comparison with Square, whether the attack strength is low or high, the ASR of the query prior-based attacks is far greater than that of Square for attacking six naturally trained models. When attacking two adversarially trained models, at the low attack strength, i.e. $\epsilon = 8/255$, some query prior-based attacks are better than Square ($Q = 10$). At the high attack strength, i.e. $\epsilon = 16/255$, Square ($Q = 10$) is better than the query prior-based attacks and Square ($Q = 0$) is better than the transfer attacks (i.e., the family of FGSMs). However, when we use the adversarially trained model as the surrogate model and reduce the query number, regardless of the attack strength is low or high, the ASR of the query prior-based attacks is greater than that of Square for attacking the other adversarially trained models.

B.3.2 Transferable priors-based black-box query attacks

We set the surrogate model as ResNet50 for CIFAR10/100 and VGG16 on ImageNet with the attack strength $\epsilon = 8/255$ to attack six naturally trained models. As shown in Tables 4, 5 and 6, by comparing the best query prior-based attacks with P-RGF, the average increase of the ASR is 86.91% for CIFAR10, 79.6% for CIFAR100 and 61.5% for ImageNet. For two adversarially trained models, the increase of the ASR is 18.6% and 13.5% for ImageNet, respectively.

We set the surrogate model as VGG16 for CIFAR10/100 and ImageNet with the attack strength $\epsilon = 16/255$ to attack six naturally trained models. As shown in Tables 7, 8 and 9, by comparing the best query prior-based attacks with P-RGF, the average increase of the ASR is 86.37% for CIFAR10, 79.21% for CIFAR100 and 68.2% for ImageNet. On two adversarially trained models, the increase of the ASR is 31.5% and 25.9% for ImageNet, respectively.

We set the surrogate model as ResNet50 for CIFAR10/100 and ImageNet with the attack strength $\epsilon = 16/255$ to attack six naturally trained models. As shown in Tables 10, 11 and 12, by comparing the best query prior-based attacks with P-RGF, the average increase of the ASR is 85.01% for CIFAR10, 75.27% for CIFAR100 and 80.5% for ImageNet. On two adversarially trained models, the increase of the ASR is 41.1% and 36.9% for ImageNet, respectively.

In conclusion, P-RGF is inefficient at limits of few queries on six naturally trained models and two adversarially trained models for CIFAR10/100 and ImageNet. The ASR of the query prior-based attacks is far greater than that of P-RGF.

B.4 Ablation study on Hyper-parameters

This section is an extension of Section 4.5 in the main paper.

B.4.1 Different numbers of the top-n wrong categories

Figure 7 evaluates the effect of different \bar{n} on the attack success rates of five naturally trained victim models and two adversarially trained victim models when these victim models are attacked by QI-FGSM ($\epsilon = 16/255$) with ResNet50 for CIFAR10/100 and ImageNet. When \bar{n} is greater than a certain threshold, the attack success rate will not be improved, e.g. the threshold is 2 for CIFAR10, 5 for CIFAR100 and 10 for ImageNet approximately. Because increasing \bar{n} increases the calculation time of the gradient, \bar{n} is not the bigger the better.

B.4.2 Different query numbers

Figure 8 evaluates the effect of different Q on the attack success rates of five naturally trained victim models and two adversarially trained victim models when these victim models are attacked by QI-FGSM ($\epsilon = 16/255$) with ResNet50 for CIFAR10/100 and ImageNet. On the victim models, the more the query, the greater the attack success rate. When the query number increases from 1 to 10, the attack success rate increases by 3% at most for CIFAR10, 8% at most for CIFAR100 and 5% at most for ImageNet approximately, and the increased attack success rate is mainly increased in the first five queries.